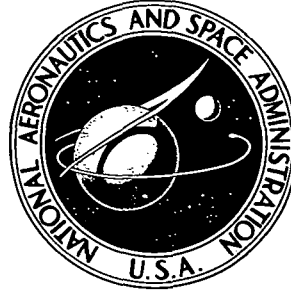# NASA CONTRACTOR REPORT

NASA CR-2255

NASA CR-2255

APPLICATION OF MATCHED ASYMPTOTIC EXPANSIONS TO LUNAR AND INTERPLANETARY TRAJECTORIES

Volume 1 - Technical Discussion

by J. E. Lancaster

Prepared by
MCDONNELL DOUGLAS ASTRONAUTICS COMPANY - WEST
Huntington Beach, Calif.
for Manned Spacecraft Center

1. Report No. NASA CR-2255	2. Government Accession No.	3. Recipient's Catalog No.
4. Title and Subtitle APPLICATION OF MATCHED ASYMPTOTIC EXPANSIONS TO LUNAR AND INTERPLANETARY TRAJECTORIES - VOLUME 1. TECHNICAL DISCUSSION		5. Report Date July 1973
		6. Performing Organization Code
7. Author(s) J. E. Lancaster		8. Performing Organization Report No. MDC G2748
		10. Work Unit No.
9. Performing Organization Name and Address McDonnell Douglas Astronautics Company - West Huntington Beach, Calif.		
		11. Contract or Grant No. NAS 9-10526
		13. Type of Report and Period Covered Contractor Report
12. Sponsoring Agency Name and Address National Aeronautics and Space Administration Washington, D.C. 20546		
		14. Sponsoring Agency Code

15. Supplementary Notes

16. Abstract

Previously published asymptotic solutions for lunar and interplanetary trajectories have been modified and combined to formulate a general analytical solution to the problem on N-bodies. The earlier first-order solutions, derived by the method of matched asymptotic expansions, have been extended to second order for the purpose of obtaining increased accuracy. The derivation of the second-order solution is summarized by showing the essential steps, some in functional form. The general asymptotic solution has been used as a basis for formulating a number of analytical two-point boundary value solutions. These include Earth-to-moon, one- and two-impulse moon-to-Earth, and interplanetary solutions. Each is presented as an explicit analytical solution which does not require iterative steps to satisfy the boundary conditions. All required formulas are presented for each solution. Comparisons between the asymptotic solutions and numerical integration are shown for several applications. The results show that the accuracies of the asymptotic solutions range from an order of magnitude better than conic approximations to that of numerical integration itself. Also, since no iterations are required, the asymptotic boundary value solutions are obtained in a fraction of the time required for comparable numerically integrated solutions. The subject of minimizing the second-order error is discussed, and recommendations made for further work directed toward achieving a uniform accuracy in all applications.

17. Key Words (Suggested by Author(s))	18. Distribution Statement Unclassified - Unlimited	
19. Security Classif. (of this report) Unclassified	20. Security Classif. (of this page) Unclassified	21. No. of Pages 112	22. Price $3.00

Acknowledgements

Preface

This report has been prepared in two volumes, each of which is a separate document. Volume 1 is in the form of the usual final report. It contains a summary of the theoretical derivations, the required analytical boundary value solutions, and a numerical analysis of the solutions, as well as con-clusions and recommendations for further work. It includes all the equations needed to evaluate any of the boundary value solutions except those equations which apply strictly to two-body motion and can be found in most standard astrodynamics or celestial mechanics textbooks.

The actual derivations of the second order asymptotic solutions are long and involved. These derivations have been compiled in a separate document which is presented as Volume 2. It contains all the assumptions and inter-mediate steps which are an important part of the theoretical development but which are not included in Volume 1. The main purpose of Volume 2 is to provide a study guide or reference for those interested in the theoretical aspects of the method of matched asymptotic expansions and/or those who may wish to modify or extend the results contained in Volume 1 to fit some particular problem.

Inasmuch as each volume was written as a separate document, there is a certain amount of overlap and cross referencing between the two. Thus the reader desiring a more detailed discussion of a particular section in Volume 1 need only refer to the corresponding section in Volume 2 and need not read through the entire theoretical analysis.

Page Intentionally Left Blank

ABSTRACT

Previously published asymptotic solutions for lunar and
interplanetary trajectories have been modified and combined to
formulate a general analytical solution to the problem on
N-bodies. The earlier first-order solutions, derived by the
method of matched asymptotic expansions, have been extended
to second order for the purpose of obtaining increased accuracy.
The derivation of the second-order solution is summarized by
showing the essential steps, some in functional form.

The general asymptotic solution has been used as a basis for
formulating a number of analytical two-point boundary value
solutions. These include Earth-to-moon, one- and two-impulse
moon-to-Earth, and interplanetary solutions. Each is presented
as an explicit analytical solution which does not require iterative
steps to satisfy the boundary conditions. All required formulas
are presented for each solution.

Comparisons between the asymptotic solutions and numerical
integration are shown for several applications. The results show
that the accuracies of the asymptotic solutions range from an
order of magnitude better than conic approximations to that of
numerical integration itself. Also, since no iterations are
required, the asymptotic boundary value solutions are obtained
in a fraction of the time required for comparable numerically
integrated solutions.

The subject of minimizing the second-order error is discussed,
and recommendations made for further work directed toward
achieving a uniform accuracy in all applications.

CONTENTS

Page Intentionally Left Blank

FIGURES

Page Intentionally Left Blank

TABLES

Section 1
INTRODUCTION

A number of approximation techniques have recently been proposed for
calculating N-body trajectories (where N is greater than two). These tech-
niques include the matched asymptotic expansion (References 1 and 2),
hybrid patched conic (Reference 3), overlapped conic (Reference 4), multi-
conic (Reference 5), virtual mass (Reference 6), slowly varying functions
(Reference 7), and Chebyeshev series (Reference 8). All these techniques
are claimed to be much faster than numerical integration and considerably
more accurate than the well known patched-conic approximation. Of all these
techniques, the matched asymptotic expansion is somewhat unique since it
represents an analytical solution to the problem of N bodies rather than just
a numerical scheme for rapid calculation. The analytical nature is useful
in solving two-point or mixed boundary value problems since, in most
instances, the solution can be obtained explicity and does not require itera-
tive steps.

The N-body problem is one of determining the motion of a body of negligible
mass subject to the gravitational forces of one primary body and N-2 second-
ary bodies. The motion of the secondary bodies relative to the primary body
is assumed to be known. In general, the dominant force on the negligible
mass body is that of the primary body. However, during a close approach
of any one of the secondary bodies there is a change in the ordering of the
dominant and perturbing forces and as a result the problem falls into a class
known as singular perturbation problems (Reference 9). An approximate
analytical solution can then be obtained by the method of matched asymptotic
expansions.

Numerical schemes give solutions to this type of problem but they require a
prescribed state vector at some time $t = t_o$ in order to uniquely define the
trajectory. In many boundary value problems the initial state vector is not

known a priori but is only partially prescribed along with some terminal conditions. The numerical schemes then require an iterative procedure to obtain the unknown part of the initial state vector, i.e., to solve the two-point boundary value problem.

The asymptotic solution can be formulated to solve the two-point boundary value problem directly, i.e., the unknown part of the initial state vector can be obtained without iterations. The solution is formulated as a set of analytical expressions in the form of asymptotic expansions. Evaluating the expressions in a certain sequence gives all the unknown parameters as functions of the prescribed boundary conditions. The goal of this study was to formulate a general, second-order asymptotic solution to the problem of N-bodies and to construct from this solution several two-point boundary value solutions. This goal can be divided into three specific objectives.

The first objective was to extend the previously published first-order solutions to second order. The results of this effort are summarized in Section 2, where the N-body differential equation of motion is used as a starting point. Section 2 covers the development of the outer and inner solutions, the overlap domain, the matching, and the fundamental solution. The latter gives the relationships between the constants of motion of the outer solution, where the primary body is dominant, and the inner solution, where one of the secondary bodies is dominant.

The fundamental solution was used to achieve the second goal of this study, the formulation of several different asymptotic two-point boundary value solutions. These solutions, which can be applied to certain classes of Earth-to-moon, moon-to-Earth, and interplanetary trajectories, are presented in Section 3. Two versions are presented for each solution, one linear, the other nonlinear. In every case at least one of the two solutions satisfies the boundary conditions exactly without iterations giving an explicit boundary value solution.

The third objective of the study was to compare the asymptotic boundary value solutions with numerical integration. Comparisons for Earth-to-moon,

two-impulse moon-to-Earth, interplanetary midcourse, and interplanetary trajectories are presented in Section 4. These results show that (1) the interplanetary solutions are more accurate than the lunar solutions, (2) midcourse solutions are more accurate than those which originate close to one body and terminate close to another, (3) the second-order solutions improve the first order in some but not all applications, and (4) the computation times for the asymptotic solutions are 6 to 150 times faster than for numerical integration.

A discussion of the conclusions obtained from this study and recommendations for further studies are contained in Section 5.

This study has focused on the application of the method of matched asymptotic expansions, and it has assumed that the reader has a certain degree of familiarity with the theoretical background. An excellent discussion of the basic theory can be found in Reference 9.

The notation used in this report is a combination of that of Lancaster (Reference 1) and Carlson (Reference 2). In general, each parameter is defined as it is introduced, but some which have only mathematical meaning and serve an intermediary role are defined only by an equation. Scalars are written as x or X and vectors as $\underline{x}$ or $\underline{X}$. A matrix $G(\underline{x})$ and a tensor $\underline{H}(\underline{x})$ are also used. In addition, a bar over a parameter indicates that it applies specifically to an inner solution. Finally, the order of a particular term in an expansion is given by the exponent of the parameter μ which precedes the term, i.e., μ^n is order n or $0(n)$.

3

Page Intentionally Left Blank

Section 2
SUMMARY OF THE ASYMPTOTIC N-BODY SOLUTION

The problem of N-bodies for which an asymptotic solution is desired consists of finding the motion of a body of negligible mass (hereinafter referred to as the particle) under the influence of one primary body and N-2 perturbing bodies whose motions relative to the primary body are known. This problem requires the solution of the differential equation

$$\ddot{\underline{r}} = \underline{f}(\underline{r}) + \underline{F}(\underline{r}, \underline{p}_i) \tag{2-1}$$

where $\underline{r}$ is the position of the particle with respect to the primary body and $\underline{p}_i$ is the position of the ith perturbing body with respect to the primary body. The functions $\underline{f}$ and $\underline{F}$ are defined by

$$\underline{f}(\underline{r}) = -\underline{r}/r^3 \tag{2-2}$$

$$\underline{F}(\underline{r}, \underline{p}_i) = \sum_{i=1}^{N-2} \mu_i \left[\underline{f}(\underline{r}-\underline{p}_i) + \underline{f}(\underline{p}_i) \right] \tag{2-3}$$

Equations (2-1) to (2-3) are dimensionless; the unit of length is the semi-major axis of the orbit of the jth body,* and the unit of time is the period of the jth body divided by 2π. In dimensionless units then the mass of the primary body is unity and of the ith body is μ_i, which is assumed to be much less than one. The origin of the coordinate system is the primary body rather than the center of mass and this gives rise to the last term in (2-3).

---

*The jth body will be termed the reference body.

For lunar trajectories the primary body is the Earth, and the two perturbing bodies of interest are the moon and the sun. (Although the μ_i for the sun is not small compared to the unit mass of the Earth, its contribution is small due to the great distance of the sun from the Earth.) For interplanetary trajectories the primary body is the sun and the perturbing bodies the planets.

As long as the particle is not close to one of the perturbing bodies, the function $\underline{F}$ in (2-1) is small compared to the other two terms. However, if a close approach is made to one of the perturbing bodies, then $\underline{F}$ becomes the dominant force and the problem falls into a class known as singular perturbation problems (Reference 9). An approximate analytical solution can then be obtained by the method of matched asymptotic expansions.

The asymptotic solution is formulated by considering two limits of (2-1) and then matching the corresponding solutions in an overlap domain. The result is termed the fundamental solution and is used to formulate the boundary value solutions in Section 3.

2.1 OUTER LIMIT

The outer limit is defined as the limit where $\underline{r} - \underline{p}_i = O(1)$ for all i. Then $\underline{F}$ is always small in (2-1), and the solution is assumed to be given by the asymptotic expansion

$$\underline{r}(t) = \underline{r}_o(t) + \mu \underline{r}_1(t) + \mu^2 \underline{r}_2(t) + O(\mu^3) \tag{2.1-1}$$

Where the reference mass μ is equal to μ_j, the dimensionless mass of the reference body. Substitution of (2.1-1) into (2-1) and equating powers of μ leads to the differential equations for $\underline{r}_o$, $\underline{r}_1$, and $\underline{r}_2$. They are

$$\ddot{\underline{r}}_o = \underline{f}(\underline{r}_o) \tag{2.1-2}$$

$$\ddot{\underline{r}}_1 = G(\underline{r}_o)\underline{r}_1 + \underline{F}_1(\underline{r}_o, \underline{p}_i) \tag{2.1-3}$$

$$\ddot{\underline{r}}_2 = G(\underline{r}_o)\underline{r}_2 + \underline{F}_2(\underline{r}_o, \underline{r}_1, \underline{p}_i) \tag{2.1-4}$$

6

where

$$\underline{F}_1 (\underline{r}_o, \underline{p}_i) = \sum_{i=1}^{N-2} M_i \left[\underline{f}(\underline{r}_o - \underline{p}_i) + \underline{f}(\underline{p}_i) \right] \qquad (2.1-5)$$

$$\underline{F}_2 (\underline{r}_o, \underline{r}_1, \underline{p}_i) = \frac{1}{2} \underline{H}(\underline{r}_o)\underline{r}_1^2 + \sum_{i=1}^{N-2} M_i G(\underline{r}_o - \underline{p}_i)\underline{r}_1 \qquad (2.1-6)$$

and

$$M_i = \mu_i / \mu \qquad (2.1-7)$$

The function $G(\underline{x})$ is a matrix defined by

$$G_{ij} = \frac{3x_i x_j}{x^5} - \frac{\delta_{ij}}{x^3} \qquad (2.1-8)$$

where δ_{ij} is the Kronecker delta. The function $\underline{H}(\underline{x})$ is a tensor defined by

$$\underline{H}_{ijk} = - \frac{15x_i x_j x_k}{x^7} + \frac{3}{x^5} (x_i \delta_{jk} + x_j \delta_{ik} + x_k \delta_{ij}) \qquad (2.1-9$$

G and $\underline{H}$ represent the first and second derivatives in the Taylor series expansion of $\underline{f}(\underline{r})$ about the nominal value $\underline{r} = \underline{r}_o$.

The solutions of (2.1-2) through (2.1-4) depend on the initial condition on $\underline{r}$ and the corresponding velocity $\underline{v}$. These initial conditions can be stated as

$$\underline{r}(t_o) = \underline{r}_o(t_o) + \mu\underline{r}_1(t_o) + \mu^2\underline{r}_2(t_o) \qquad (2.1-10)$$

$$\underline{v}(t_o) = \underline{v}_o(t_o) + \mu\underline{v}_1(t_o) + \mu^2\underline{v}_2(t_o) \qquad (2.1-11)$$

Then the solutions are

$$\underline{r}_0(t) = f_0(t)\underline{r}_0(t_o) + g_0(t)\underline{v}_0(t_o) \tag{2.1-12}$$

$$\underline{r}_1(t) = A(t, t_o)\underline{r}_1(t_o) + B(t, t_o)\underline{v}_1(t_o) + \int_{t_o}^{t} B(t, \tau) \underline{F}_1(\tau)d\tau \tag{2.1-13}$$

$$\underline{r}_2(t) = A(t, t_o)\underline{r}_2(t_o) + B(t, t_o)\underline{v}_2(t_o) + \int_{t_o}^{t} B(t, \tau) \underline{F}_2(\tau)d\tau \tag{2.1-14}$$

The solution for $\underline{r}_0$ is the standard two-body ellipse resulting from the two-body differential equation (2.1-2). The functions f_0 and g_0 are infinite series in time or can be written in closed form using eccentric anomaly as the independent variable. They are defined in any standard astrodynamics textbook and in References 2 and 10.[*] The solutions for $\underline{r}_1$ and $\underline{r}_2$ are made up of a homogeneous solution which is simply the propagation of initial deviations along the two-body solution $\underline{r}_0$, and a particular integral which introduces the perturbations from two-body motion. The functions $A(t, t_o)$ and $B(t, t_o)$ are partial derivative matrices which arise by partitioning the state transition matrix

$$\Phi(t, t_o) = \begin{pmatrix} \dfrac{\partial \underline{r}_0(t)}{\partial \underline{r}_0(t_o)} & \dfrac{\partial \underline{r}_0(t)}{\partial \underline{v}_0(t_o)} \\[1em] \dfrac{\partial \underline{v}_0(t)}{\partial \underline{r}_0(t_o)} & \dfrac{\partial \underline{v}_0(t)}{\partial \underline{v}_0(t_o)} \end{pmatrix} = \begin{pmatrix} A(t, t_o) & B(t, t_o) \\[1em] C(t, t_o) & D(t, t_o) \end{pmatrix} \tag{2.1-15}$$

---

[*]Reference 10 has been included as a second volume of this report. It is hereinafter referred to only as Volume 2.

8

Many expressions have been derived for the partial derivative matrices in various coordinate systems. Some are discussed in Reference 2 and in Volume 2.

The solutions given by (2.1-12) through (2.1-14) can be substituted back into (2.1-1) giving a second-order solution for the position $\underline{r}$ of the particle. The solution is a function only of the initial conditions (2.1-10) and (2.1-11) and the time histories of the perturbing bodies $\underline{p}_i$. The initial conditions can be chosen so that at some time $t = t_k$ the trajectory passes close to the kth body. This introduces another limit.

The outer solution and its behavior as t approached t_k are shown in Figure 1.

2.2 INNER LIMIT

The inner limit is defined as the limit where $\underline{r} - \underline{p}_k = 0(\mu_k)$ for some k. This limit arises when the particle makes a close approach to the kth body. This limit requires the change of variables

CR17
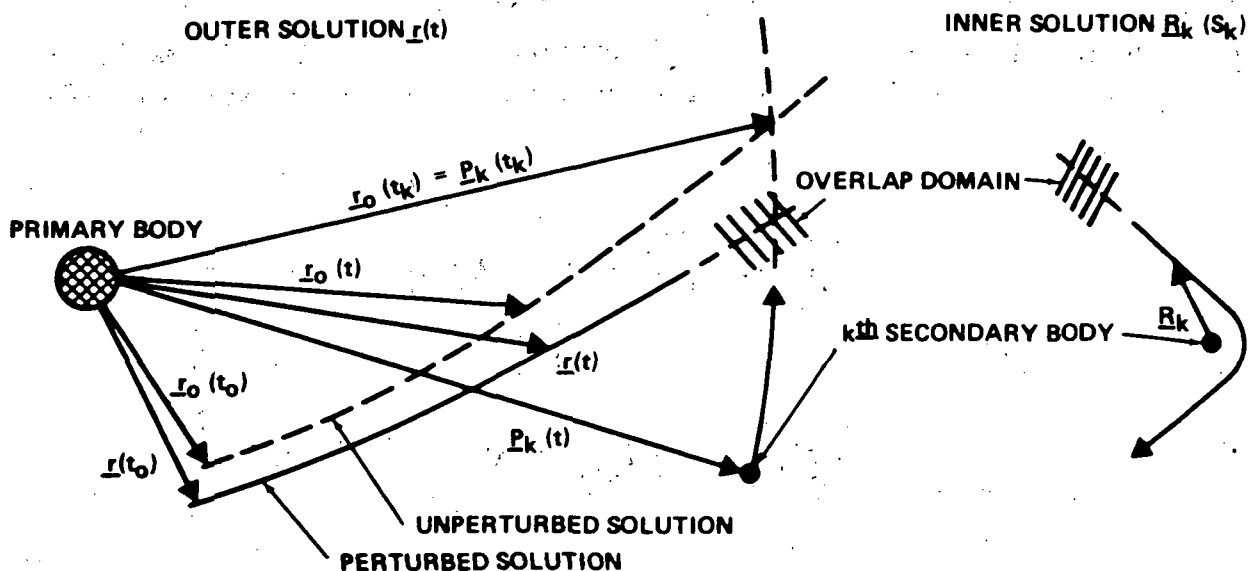
Figure 1. Outer Solution, Inner Solution, and Overlap Domain

$$\underline{R}_k = (\underline{r} - \underline{p}_k)/\mu_k \qquad (2.2\text{-}1)$$

$$S_k = (t - t_{pk})/\mu_k \qquad (2.2\text{-}2)$$

where $\underline{p}_k$ is the position of the $k^{\underline{th}}$ body and t_{pk} is the time of pericenter passage of the trajectory about the $k^{\underline{th}}$ body. The latter can be written

$$t_{pk} = t_k + \mu_k \tau_k \qquad (2.2\text{-}3)$$

and t_k chosen as the time at which the two-body outer solution $\underline{r}_o$ passes through the center of the $k^{\underline{th}}$ body, i.e., at $t = t_k$

$$\underline{r}_o(t_k) = \underline{p}_k(t_k) \qquad (2.2\text{-}4)$$

Substitution of the inner variables (2.2-1) and (2.2-2) into (2-1) gives the inner differential equation

$$\frac{d^2 \underline{R}_k}{dS_k^2} = \underline{f}(\underline{R}_k) + \underline{P}(\underline{R}_k, \underline{p}_k, \underline{p}_i) \qquad (2.2\text{-}5)$$

where $\underline{P}$ is a function defined in Volume 2. If the expansion

$$\underline{R}_k(S_k) = \underline{R}_{ko}(S_k) + \mu_k \underline{R}_{k1}(S_k) + \mu_k^2 \underline{R}_{k2}(S_k) + O(\mu_k^3) \qquad (2.2\text{-}6)$$

is substituted into (2.2-5) and powers of μ_k equated the differential equations are

$$\frac{d^2 \underline{R}_{ko}}{dS_k^2} = \underline{f}(\underline{R}_{ko}) \qquad (2.2\text{-}7)$$

$$\frac{d^2 \underline{R}_{k1}}{dS_k^2} = 0 \qquad (2.2\text{-}8)$$

$$\frac{d^2 \underline{R}_{k2}}{dS_k^2} = G(\underline{R}_{ko})\underline{R}_{k2} + G(\underline{p}_k(t_k))\underline{R}_{ko} \tag{2.2-9}$$

The solutions of (2.2-7) through (2.2-9) depend on the initial conditions on $\underline{R}_k$ and the corresponding velocity $\underline{V}_k$. These initial conditions can be stated as

$$\underline{R}_k(S_{ko}) = \underline{R}_{ko}(S_{ko}) \tag{2.2-10}$$

$$\underline{V}_k(S_{ko}) = \underline{V}_{ko}(S_{ko}) \tag{2.2-11}$$

These initial conditions assume that the perturbations vanish at $S_k = S_{ko}$ and that the full solution (2.2-6) can be represented by $\underline{R}_{ko}$ at this point. As a result the solutions are

$$\underline{R}_{ko}(S_k) = \overline{f}_o(S_k)\underline{R}_{ko}(S_{ko}) + \overline{g}_o(S_k)\underline{V}_{ko}(S_{ko}) \tag{2.2-12}$$

$$\underline{R}_{k1}(S_k) = 0 \tag{2.2-13}$$

$$\underline{R}_{k2}(S_k) = \int_{S_{ko}}^{S_k} \overline{B}(S_k, \xi)G(\underline{p}_k(t_k))\underline{R}_{ko}(\xi)d\xi \tag{2.2-14}$$

The solution for $\underline{R}_{ko}$ is the standard two-body hyperbola resulting from the two-body differential equation (2.2-7). The functions $\overline{f}_o$ and $\overline{g}_o$ are defined in many textbooks and in Volume 2. Like their counterparts in the elliptical solution of the previous section, they can be written in closed form using hyperbolic eccentric anomaly as the independent variable. The function $\overline{B}(S_k, \xi)$ is the partial derivative matrix

$$\overline{B}(S_k, \xi) = \frac{\partial \underline{R}_{ko}(S_k)}{\partial \underline{V}_{ko}(\xi)} \tag{2.2-15}$$

11

The solutions given by (2.2-12) through (2.2-14) can be substituted back into (2.2-6) giving a second-order solution for $\underline{R}_k$. The solution is shown in Figure 1.

2.3 OVERLAP DOMAIN

The outer and inner solutions are functions of the vector constants given by (2.1-11), (2.1-12), (2.2-10), and (2.2-11). For a trajectory which is continuous from the domain of the outer solution to the domain of the inner solution, these constants are not all independent. In a region designated as the overlap domain, the outer and inner solutions must exhibit certain similarities, i.e., both solutions must represent the trajectory in this domain. This characteristic makes it possible to determine explicit relationships between the constants of the two solutions. A representation of the overlap domain is shown in Figure 1.

The overlap domain is defined as the domain of the intermediate limit, i.e., the domain where $t-t_{pk} = 0(\mu^{\alpha})$ with $0<\alpha<1$. This limit is formally defined by introducing the intermediate variable

$$\sigma_k = (t-t_{pk})/\mu_k^{\alpha} \qquad 0 \le \alpha_0 <\alpha <\alpha_1 \le 1 \qquad (2.3-1)$$

If $\alpha = 0$ then (2.3-1) simply shifts the time scale of the outer solution to a new origin. If $\alpha = 1$, $\sigma_k = S_k$ giving the inner time. Within the range $\alpha_0 <\alpha <\alpha_1$, σ_k is then intermediate to the outer and inner times. The values of α_0 and α_1 must be determined from the matching.

The outer solution is a function of t and replacing t_{pk} in (2.3-1) by (2.2-3) and solving for $t-t_k$ gives

$$t-t_k = \mu_k^{\alpha}\sigma_k + \mu_k \tau_k \qquad (2.3-2)$$

Since μ_k is small, (2.3-2) indicates that the outer solution must be expanded to about $t = t_k$ in order to determine its behavior in the overlap domain. This expansion is derived in Section A11 of Volume 2.

12

The outer expansion can be summarized in function form by the following expression:

$$\underline{r} = \underline{r}(t-t_k, \mu; \underline{r}(t_o), \underline{v}(t_o); \underline{Y}_k^*, \underline{\delta}_k^*, \underline{\zeta}_k^*, \underline{\eta}_k^*) \qquad (2.3-3)$$

The position vector $\underline{r}$, when $t-t_k$ is small, is a function of both the initial conditions at t_o and four constants, $\underline{Y}_k^*$, $\underline{\delta}_k^*$, $\underline{\zeta}_k^*$, and $\underline{\eta}_k^*$, which represent the first- and second-order deviations from two-body motion over the interval $t_o \leq t \leq t_k$. These constants are discussed in detail in Subsection 3.8.

The inner solution is a function of S_k and comparing (2.3-1) with (2.2-2) yields

$$S_k = \mu_k^{\alpha-1} \sigma_k \qquad (2.3-4)$$

Since $\alpha - 1 < 0$, (2.3-3) indicates that the inner solution must be expanded for S_k large. This expansion is derived in Section A12 of Volume 2.

The inner expansion can be summarized in functional form by the following expression:

$$\underline{R}_k = \underline{R}_k(S_k, \mu_k; \underline{V}_{\infty k}, \underline{L}_k; \underline{A}_{k2}^*) \qquad (2.3-5)$$

The position vector $\underline{R}_k$, when S_k is large, is a function of $\underline{V}_{\infty k}$, the hyperbolic excess velocity, $\underline{L}_k$ a vector function of the orbital elements, and $\underline{A}_{k2}^*$, which represents the second-order deviation from two-body motion far out on the asymptote of the zeroth-order hyperbola. These constants are discussed further in Subsection 3.8.

It is also necessary to expand the motion of the $k^{\underline{th}}$ body when $t-t_k$ is small. The expansion is obtained by a Taylor series in Section A11 of Volume 2. It may be summarized simply as the function

$$\underline{p}_k = \underline{p}_k(t-t_k) \qquad (2.3-6)$$

13

2.4 MATCHING

For the outer and inner solutions to match, they must be in terms of a common independent variable. The expansion of the outer solution near $t = t_k$, summarized by (2.3-3), can be written in terms of σ_k and μ_k using (2.3-2) giving

$$\underline{r} = \underline{r}(\mu_k^\alpha \sigma_k + \mu_k \tau_k, \mu; \underline{r}(t_o), \underline{v}(t_o); \underline{Y}_k^*, \underline{\delta}_k^*, \underline{\zeta}_k^*, \underline{\eta}_k^*) \equiv \underline{\phi}_1 \qquad (2.4-1)$$

The position $\underline{r}$ in terms of the inner solution $\underline{R}_k$ is found from (2.2-1), i.e.,

$$\underline{r} = \underline{p}_k + \mu_k \underline{R}_k \qquad (2.4-2)$$

The expansion for the position of the $k\underline{\text{th}}$ body near $t = t_k$, given by (2.3-6), can also be written in terms of σ_k and μ_k giving

$$\underline{p}_k = \underline{p}_k(\mu_k^\alpha \sigma_k + \mu_k \tau_k) \equiv \underline{\phi}_2 \qquad (2.4-3)$$

Finally the expansion for $\underline{R}_k$ when S_k is large, obtained from (2.3-5), can be written in terms of σ_k and μ_k using (2.3-3) giving

$$\underline{R}_k = \underline{R}_k(\mu_k^{\alpha-1} \sigma_k, \mu_k; \underline{V}_{\infty k}, \underline{L}_k; \underline{A}_{k2}^*) \equiv \underline{\phi}_3 \qquad (2.4-4)$$

Substituting (2.4-3) and (2.4-4) into (2.4-2) gives

$$\underline{r} = \underline{\phi}_2 + \mu_k \underline{\phi}_3 \qquad (2.4-5)$$

Simply stated, the matching requires that the difference between the outer solution, as given by (2.4-1), and the inner solution, as given by (2.4-5), must be vanishingly small in some appropriate limit. Cole (Reference 9) states this limit as

$$\lim_{\substack{\mu_k \to 0 \\ \sigma_k \text{ constant}}} \left[\frac{\phi_1 - \phi_2 - \mu_k \phi_3}{\epsilon(\mu_k)} \right] = 0 \qquad (2.4\text{-}6)$$

where $\epsilon(\mu_k)$ is a gauge function. For a second-order theory $\epsilon(\mu_k)$ is most easily chosen to be μ_k^2.

In Section A14 of Volume 2, it is shown that this limit exists only if

$$\alpha_0 = 2/5 \qquad (2.4\text{-}7)$$

$$\alpha_1 = 1/2 \qquad (2.4\text{-}8)$$

Thus the overlap domain is a region of order μ^a where $2/5 < a < 1/2$ and $a = 1/2$ is not included. This is a result of the second-order solution inasmuch as Carlson (Reference 2) showed that the first-order solution can be matched with $a = 1/2$.

This was an assumption in his derivation and not a result of applying a rigorous matching requirement such as (2.4-6). The present results show that his approach to matching will not work for second order, i.e., certain terms which are singular in the limit (2.4-6) can only be eliminated if $a < 1/2$.

2.5 FUNDAMENTAL SOLUTION

The complete matching process is discussed in Sections A14 to A17, and Section B1 of Volume 2. The result, summarized in one six-component state vector equation which will be called the fundamental solution, is

$$\begin{pmatrix} \underline{r}_1(t_o) + \mu \underline{r}_2(t_o) \\ \underline{v}_1(t_o) + \mu \underline{v}_2(t_o) \end{pmatrix} = \Phi(t_o, t_k) \left\{ \begin{pmatrix} \mathcal{L}_k \\ \mu^{-1}(\underline{V}_{\infty k} - \underline{V}_k) \end{pmatrix} + \begin{pmatrix} \underline{\gamma}_k + \mu \underline{\zeta}_k \\ \underline{\delta}_k + \mu \underline{\eta}_k \end{pmatrix} \right\} \qquad (2.5\text{-}1)$$

where

$$\underline{\mathcal{L}}_k = M_k \left\{ \underline{L}_k - \left[\tau_k + \frac{Q_k}{\bar{n}_k} \log \left(\frac{\mu_k \bar{e}_k}{2\bar{n}_k} \right) \right] \underline{V}_{\infty k} \right\} \qquad (2.5\text{-}2)$$

$$\underline{Y}_k = \underline{Y}_k^* \qquad (2.5\text{-}3)$$

$$\underline{\delta}_k = \underline{\delta}_k^* \qquad (2.5\text{-}4)$$

$$\underline{\zeta}_k = \underline{\zeta}_k^* \qquad (2.5\text{-}5)$$

$$\underline{\eta}_k = \underline{\eta}_k^* + \underline{A}_{k2}^* \qquad (2.5\text{-}6)$$

and, except in the log term, μ_k has been eliminated in favor of the reference mass μ (which may be equal to μ_k if the $k\underline{\text{th}}$ body is also the reference body used to non-dimensionalize the differential equations).

Equation (2.5-1) is a relation between the constants of the outer and inner solutions. The only constants which do not appear explicitly are the initial position and velocity of the zeroth-order outer solution, $\underline{r}_o(t_o)$ and $\underline{v}_o(t_o)$. They must be chosen to make the zeroth-order ellipse intersect the position of the $k\underline{\text{th}}$ body at $t = t_k$, i. e. , to satisfy (2.2-4). They then enter implicitly through the relative velocity $\underline{V}_k$ which is the difference between the zeroth-order velocity and the velocity of the $k\underline{\text{th}}$ body at $t = t_k$ (and should not be confused with the inner, time-dependent velocity $\underline{V}_k(S_k)$).

Equation (2.5-1) can be used to solve either initial or boundary value problems. The initial value solution is discussed in Section A of Volume 2. It is the boundary value solution which is of interest in this study, and the applications of (2.5-1) are discussed in the following subsections.

2.6 COMMENTS

The asymptotic solution presented here is similar, when second-order terms are ignored, to the first-order solution derived by Carlson (Reference 2). The obvious differences between the two first-order solutions are (1) the use of dimensionless variables, (2) isolating the small parameter μ so that it appears explicitly, and (3) using the vector $\underline{L}_k$ as one of the constants of the inner solution rather than the standard impact parameter vector.

The two solutions are numerically equivalent when applied to an initial value problem. However, using the vector $\underline{L}_k$, does result in a mathematically different solution when the fundamental solution is applied to boundary value problems. This is because the use of the impact parameter vector results in boundary value solutions which satisfy the boundary conditions in a "best" sense while the $\underline{L}_k$ vector results in solutions satisfying the boundary conditions exactly. The two vectors are related by (cf. Volume 2)

$$\underline{b}_k = \underline{L}_k + (Q_k / \bar{n}_k) \, \underline{V}_{\infty k} \qquad (2.6-1)$$

where Q_k and $\bar{n}_k$ are defined in Subsection 3.8.

Next, it should be noted that the second-order terms add considerable complexity to the solution although such complexity is not apparent in this section. Some of the complexity can be seen from the formulas in Subsection 3.8, but it is necessary to follow the derivation in Volume 2 to really appreciate just how much complexity is actually added. The amount of algebra necessary to extend the solution to a higher order would probably be prohibitive and the result somewhat unmanageable. The first-order solution contains the 3x3 gravity gradient matrix G, while the second-order solution contains the 3x3x3 tensor $\underline{H}$. Each succeeding order adds a tensor of higher order. If the dimensions of the tensor are used as a measure of the complexity of the solution, then an nth order solution has a complexity of order 3^{n+1}.

Finally, it should be pointed out that the form of the fundamental solution is not unique. The matching results contained in the fundamental solution are similar, but not identical, to those of Carlson (Reference 2). Differences which are not immediately obvious are due to the fact that an asymptotic expansion of a given function is not unique. Other expansions can be formulated to represent the same function but actually appear as different expansions. When the individual expressions which result from the matching are combined to form the fundamental solution, there are several ways in which such a combination can occur. Thus for a second-order solution the error in each case may be order μ^3, but the actual value of the error may differ, i.e., for one case it may be $3\mu^3$ while for another case it may be $0.5\mu^3$. This aspect is discussed further in Subsection 4.6.

Section 3

ASYMPTOTIC BOUNDARY VALUE SOLUTIONS

The boundary value solutions presented in this section are of three general types: (1) trajectories which originate at some known position relative to the primary body and terminate at a fixed pericenter radius, inclination, and time at one of the perturbing bodies (cf., Subsections 3.2, 3.3, and 3.6), (2) trajectories which originate at some known position close to one of the perturbing bodies and terminate close to the primary body with fixed entry conditions (cf., Subsections 3.4 and 3.5), and (3) trajectories which originate close to one perturbing body and terminate close to another with fixed pericenter radius, inclination, and time at each end (cf., Subsection 3.7).

Each of the boundary value solutions evolves from (2.5-1),* and each requires at least one solution of a Lambert problem to establish the zeroth-order outer solution. The two types of Lambert solutions which are required are discussed in Subsection 3.1. Subsections 3.2 through 3.7 present the various boundary value solutions, and finally Subsection 3.8 gives formulas for evaluating all the constants which appear in the boundary value solutions.

The sections which follow contain only the end results of the boundary value solutions. More detailed discussions and the steps necessary to go from (2.5-1) to each solution are contained in Volume 2.

3.1 THE LAMBERT PROBLEM

The standard Lambert problem is one of finding the two-body solution which connects two known position vectors in a fixed time of flight. If the two

---

*Except for the two-impulse moon-to-Earth solution for which two different types of solutions have been derived, one of which does not evolve from (2.5-1). It is this latter solution which is presented in Subsection 3.5.

position vectors are $\underline{x}_1$ and $\underline{x}_2$ and the time of flight t_f, then Lambert's theorem states that

$$t_f = t_f(a, \ x_1 + x_2, \ c) = t_2 - t_1 \qquad (3.1-1)$$

where a is the semimajor axis which is unknown and c is the chord length between $\underline{x}_1$ and $\underline{x}_2$. The chord length is found from the law of cosines, i.e.,

$$c^2 = x_1^2 + x_2^2 + 2x_1 x_2 \cos \theta_{12} \qquad (3.1-2)$$

where θ_{12} is the central angle between $\underline{x}_1$ and $\underline{x}_2$.

An iterative solution is required to determine the semimajor axis. Once it is known, the velocities $\underline{\dot{x}}_1$ and $\underline{\dot{x}}_2$ and the solution $\underline{x}(t)$ can be obtained. Many techniques have been proposed for solving the Lambert problem. One such method is discussed by Battin (Reference 11).

The standard Lambert problem requires that the two vectors $\underline{x}_1$ and $\underline{\dot{x}}_2$ be given. The zeroth-order solutions used in the Earth-to-moon and interplanetary solutions are of this type. The zeroth-order moon-to-Earth solutions however do not rely on a given position vector at the Earth. Instead, entry conditions of radius and flight path angle are prescribed at a given time. In addition, the trajectory is to satisfy a prescribed inclination. The solution for the semimajor axis is now more difficult, since θ_{12} in (3.1-2) is not known a priori. This angle is the difference between the true anomalies at the endpoints, i.e.,

$$\theta_{12} = f_2 - f_1 \qquad (3.1-3)$$

where

$$f_1 = \cos^{-1} \left[\frac{a(1 - e^2) - x_1}{ex_1} \right] \qquad (3.1-4)$$

20

$$f_2 = \cos^{-1}\left[\frac{a(1-e^2) - x_2}{ex_2}\right] \quad . \quad (3.1\text{-}5)$$

The eccentricity e is a function of a, x_2 and the flight path angle γ_2, measured from the local horizontal. The relationship is

$$e = \left[a^2 + x_2(x_2 - 2a)\cos^2\gamma_2\right]^{1/2}/a \quad (3.1\text{-}6)$$

The modified Lambert problem requires the simultaneous solution of (3.1-1) through (3.1-6) for a, c, θ_{12}, f_1, f_2 and e. Once these parameters are determined they, along with the prescribed inclination, are sufficient to solve for the velocities $\underline{\dot{x}}_1$ and $\underline{\dot{x}}_2$ and the time-dependent solution $\underline{x}(t)$. The solution is discussed in detail in Section B4.1 of Volume 2, and a similar problem is discussed in Reference 11.

3.2 EARTH-TO-MOON SOLUTION

The Earth-to-moon problem is one in which the target body is the moon. The moon should also be the reference body, therefore

$$k = M \quad (3.2\text{-}1)$$

$$\mu = \mu_M \quad (3.2\text{-}2)$$

The simplest Earth-to-moon boundary value problem is shown in Figure 2. The initial time, t_o, the initial position relative to the earth, $\underline{r}(t_o)$, and the pericynthion radius, $\bar{\rho}_M$, inclination, $\bar{i}_M$, and time, t_{PM}, are all prescribed. The initial velocity relative to the earth, $v(t_o)$, is unknown and must be determined from the fundamental solution. In order to evaluate the solution, an ephemeris is required giving the position and velocity of the moon and the position of the sun in Cartesian coordinates with origin at the Earth.
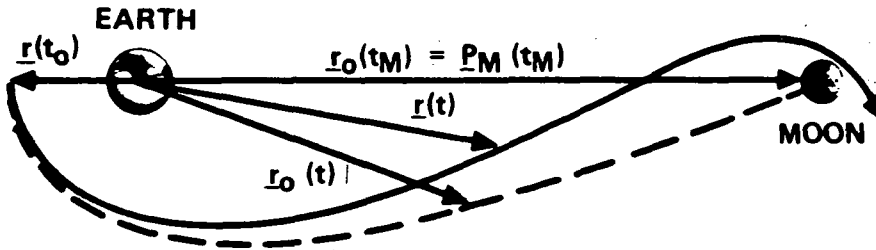
Figure 2. Earth-to-Moon Solution

From Figure 2 it can be seen that the zeroth-order ellipse, $r_o(t)$, coincides with the higher order solution, $r(t)$, at $t = t_o$. Therefore, in (2.1-10) let

$$\underline{r}_1(t_o) = \underline{r}_2(t_o) = 0 \tag{3.2-3}$$

Then

$$r_o(t_o) = \underline{r}(t_o) \tag{3.2-4}$$

defining the initial position of the zeroth-order ellipse.

From (2.2-3)

$$t_M = t_{PM} - \mu \tau_M \qquad (3.2-5)$$

where τ_M is arbitrary and can be put equal to zero without loss of generality. Non-zero values of τ_M simply cause a change in t_M when t_{PM} is held constant. The final position of the zeroth-order ellipse comes from (2.2-4)

$$\underline{r}_o(t_M) = \underline{p}_M(t_M) \qquad (3.2-6)$$

where $\underline{p}_M$ is the position of the moon obtained from the ephemeris. The two position vectors, $\underline{r}_o(t_o)$ and $\underline{r}_o(t_M)$, define a standard Lambert problem of the type discussed in Subsection 3.1. Solution of the problem gives $\underline{r}_o(t)$, shown as the dashed line in Figure 2, and the initial and final zeroth-order velocities, $\underline{v}_o(t_o)$ and $\underline{v}_o(t_M)$. The latter is used to define the relative velocity

$$\underline{V}_M = \underline{v}_o(t_M) - \underline{\dot{p}}_M(t_M) \qquad (3.2-7)$$

where $\underline{\dot{p}}_M$ is the velocity of the moon.

Now let the initial velocity perturbation be

$$\delta \underline{v}(t_o) = \underline{v}_1(t_o) + \mu \, \underline{v}_2(t_o) \qquad (3.2-8)$$

Then the initial velocity at t_o is

$$\underline{v}(t_o) = \underline{v}_o(t_o) + \mu \, \delta \underline{v}(t_o) \qquad (3.2-9)$$

while the excess velocity at the moon can be written

$$\underline{V}_{\infty M} = \underline{V}_M + \mu \, \delta \underline{V}_\infty \qquad (3.2-10)$$

The perturbation terms in (3.2-9) and (3.2-10) are obtained from the fundamental solution. They are

$$\delta \underline{v}(t_o) = B(t_M, t_o)^{-1} (\underline{\mathscr{X}}_M + \underline{Y}_M + \mu \underline{\zeta}_M) \qquad (3.2-11)$$

$$\delta \underline{V}_\infty = D(t_M, t_o) \delta \underline{v}(t_o) - \underline{\delta}_M - \mu \underline{n}_M \qquad (3.2-12)$$

Equations (3.2-9) through (3.2-12) constitute a linear solution to the boundary value problem.

Since $\underline{V}_{\infty M}$ enters (3.2-11) through $\underline{\mathscr{X}}_M$ and since $\delta \underline{v}(t_o)$ appears in (3.2-12) they are not explicit relations but must be solved in a sequence using the zeroth-, first-, and second-order terms successively. The zeroth-order approximation is obtained by putting $\mu = 0$ in (3.2-9) and (3.2-10). The first-order approximation is obtained by putting $\mu = 0$ in (3.2-11) and (3.2-12) and using the zeroth-order value of $\underline{V}_{\infty M}$ to evaluate (3.2-11). The second-order approximation is obtained by evaluating (3.2-11) and (3.2-12) with $\mu \neq 0$ and using the first-order $\underline{V}_{\infty M}$ in (3.2-11).

Combining (3.2-9) with the prescribed value of $\underline{r}(t_o)$ gives a complete set of initial conditions for a trajectory satisfying all the conditions of the boundary value problem. Combining (3.2-10) with the prescribed values of pericynthion radius and inclination gives a complete set of terminal conditions as shown in Subsection 3.8.

An alternate solution, called the nonlinear solution (Reference 2), can be obtained from the solutions of a sequence of Lambert problems defined by the position vectors

$$\underline{r}'_o(t_o) = \underline{r}_o(t_o) \qquad (3.2-13)$$

$$\underline{r}'_o(t_M) = \underline{r}_o(t_M) + \mu \delta \underline{r}(t_M) \qquad (3.2-14)$$

where

$$\delta \underline{r}(t_M) = \underline{\mathcal{L}}_M + \underline{Y}_M + \mu \underline{\zeta}_M \qquad (3.2\text{-}15)$$

Solution of the Lambert problems gives the initial and final velocities, $\underline{v}_o'(t_o)$ and $\underline{v}_o'(t_M)$. Then the initial velocity replacing (3.2-9) is

$$\underline{v}(t_o) = \underline{v}_o'(t_o) \qquad (3.2\text{-}16)$$

and the excess velocity replacing (3.2-10) is

$$\underline{V}_{\infty M} = \underline{V}_M' + \mu \delta \underline{V}_\infty' \qquad (3.2\text{-}17)$$

where

$$\underline{V}_M' = \underline{v}_o'(t_M) - \underline{\dot{p}}_M(t_M) \qquad (3.2\text{-}18)$$

$$\delta \underline{V}_\infty' = -\underline{\delta}_M - \mu \underline{\eta}_M \qquad (3.2\text{-}19)$$

Again the solution requires a sequence of steps. The zeroth-order approximation is obtained by putting $\mu = 0$ is (3.2-14) and (3.2-17) and is identical to the zeroth-order linear solution. The first-order approximation is obtained by putting $\mu = 0$ in (3.2-15) and (3.2-19) and using the zeroth-order $\underline{V}_{\infty M}$ in (3.2-15). And the second-order approximation is obtained by using the first-order $\underline{V}_{\infty M}$ in (3.2-15). The nonlinear solution is shown in Figure 3.

The first- and second-order nonlinear solutions will be slightly different from their linear counterparts since they include nonlinear effects in the zeroth-order solution which are not contained in the B and D partial derivative matrices used in the linear solutions.
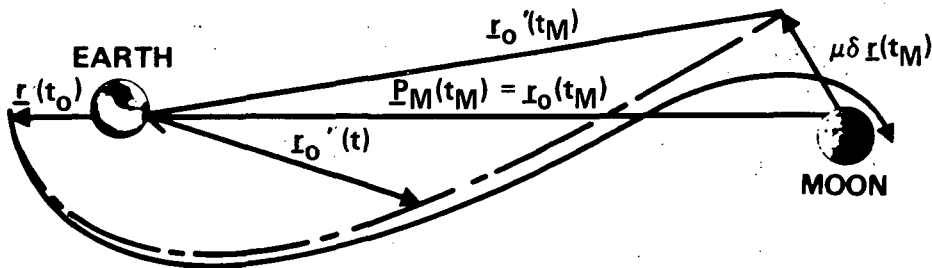
Figure 3. Nonlinear Version of Earth-to-Moon Solution

The constants $\underline{Y}_M$, $\underline{\delta}_M$, $\underline{\zeta}_M$ and $\underline{\eta}_M$ are fixed through each step of both the linear and nonlinear solutions. The function $\underline{\mathscr{X}}_M$, however, depends on $\underline{V}_{\infty M}$ and must be evaluated for each of the zeroth- , first- , and second-order approximations. Formulas for calculating all of the constants are in Subsection 3.8.

3.3 EARTH-TO-MOON MIDCOURSE SOLUTION

In the previous section, the initial position, $\underline{r}(t_o)$, was implicitly assumed to be close to the Earth. The same analysis may also be used for a midcourse maneuver where the position, $\underline{r}(t_o)$, represents a point between the Earth and the moon, as shown in Figure 4. The velocity just prior to the midcourse maneuver is $\underline{v}(t_o^-)$ and after the maneuver it is $\underline{v}(t_o^+)$. Therefore, the midcourse velocity correction is

$$\Delta \underline{v}(t_o) = \underline{v}(t_o^+) - \underline{v}(t_o^-)$$

$$= \underline{v}_o(t_o^+) - \underline{v}(t_o^-) + \mu \, \delta \underline{v}(t_o^+) \qquad (3.3-1)$$

26
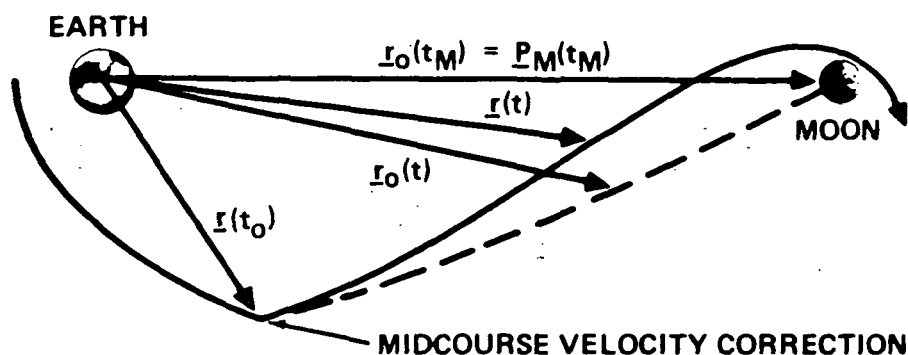
Figure 4. Earth-to-Moon Midcourse Solution

The solution of Subsection 3.2 can be used to calculate $\underline{v}_o(t_o^+)$ and $\delta\underline{v}(t_o^+)$ and since $\underline{r}(t_o)$ and $\underline{v}(t_o^-)$ are known, (3.3-1) gives an analytical expression for the midcourse velocity correction.

3.4 ONE-IMPULSE MOON-TO-EARTH SOLUTION

In the moon-to-Earth problem, the moon becomes the launch body and is also the reference body. Therefore, as in Subsection 3.2,

$$k = M \tag{3.4-1}$$

$$\mu = \mu_M \tag{3.4-2}$$

The boundary value problem is shown in Figure 5. The initial time, t_1, the initial position relative to the moon, $\underline{R}_{M1}$, and the entry time, t_e, radius, r_e, flight path angle, γ_e, and inclination, i_e, are all prescribed. The initial velocity relative to the moon, $\underline{V}_{M1}$, is unknown and must be
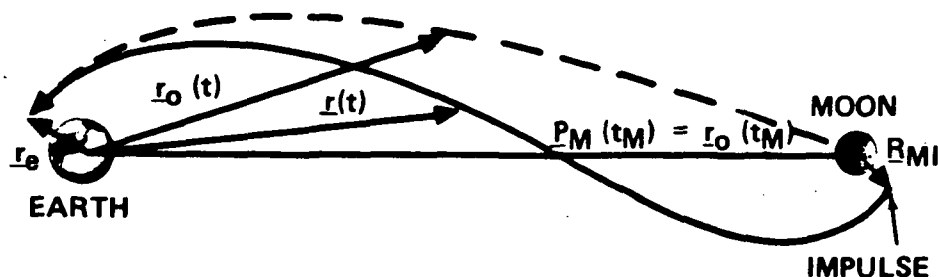
Figure 5. One-Impulse Moon-to-Earth Solution

determined using the fundamental solution. An ephemeris like that used for the Earth-to-moon solution is required.

Since entry conditions rather than a fixed position vector are prescribed at Earth, this solution requires the solution of the modified Lambert problem discussed in Section 3.1. The initial position of the zeroth-order ellipse comes from (2.2-4)

$$\underline{r}_o(t_M) = \underline{p}_M(t_M) \qquad (3.4-3)$$

where $\underline{p}_M$ is the position of the moon obtained from the ephemeris and, for convenience,

$$t_M = t_1 \qquad (3.4-4)$$

The final position $\underline{r}_o(t_e)$ must be determined from the solution of the modified Lambert problem along with $\underline{r}_o(t)$, shown as the dashed line in Figure 5, and the initial and final zeroth-order velocities, $\underline{v}_o(t_M)$ and $\underline{v}_o(t_e)$. The initial zeroth-order velocity is used to define the relative velocity

$$\underline{V}_M = \underline{v}_o(t_M) - \underline{\dot{p}}_M(t_M) \qquad (3.4-5)$$

where $\underline{\dot{p}}_M$ is the velocity of the moon.

The zeroth-order solution satisfies the entry conditons exactly, therefore any perturbations at $t = t_e$ will cause the trajectory to deviate slightly from the prescribed conditions. As shown in Figure 5, the position perturbation can be made to vanish, i.e.,

$$\underline{r}_1(t_o) = \underline{r}_2(t_o) = 0 \qquad (3.4-6)$$

so that

$$\underline{r}(t_o) = \underline{r}_o(t_o) \qquad (3.4-7)$$

The velocity perturbation cannot vanish without overly constraining the problem, therefore,

$$\delta \underline{v}(t_e) = \underline{v}_1(t_e) + \mu \, \underline{v}_2(t_e) \neq 0 \qquad (3.4-8)$$

so that entry velocity is

$$\underline{v}(t_e) = \underline{v}_o(t_e) + \mu \delta \underline{v}(t_e) \qquad (3.4-9)$$

The hyperbolic excess velocity is given by

$$\underline{V}_{\infty M} = \underline{V}_M + \mu \delta \underline{V}_\infty \qquad (3.4-10)$$

The perturbation terms in (3.4-9) and (3.4-10) are obtained from the fundamental solution. They are

$$\delta \underline{v}(t_e) = B(t_M, t_e)^{-1} (\underline{\mathscr{X}}_M + \underline{Y}_M + \mu \underline{\zeta}_M) \qquad (3.4-11)$$

$$\delta \underline{V}_\infty = D(t_M, t_e) \, \delta v(t_e) - \underline{\delta}_M - \mu \, \underline{\eta}_M \qquad (3.4-12)$$

Using the initial position $\underline{R}_{M1}$ and the excess velocity $\underline{V}_{\infty M}$, a new parameter X_M is defined by

$$X_M = 1 + 4 \left\{ R_{M1} \, V_{\infty M}^2 \left[1 + \cos \left(\frac{\underline{R}_{M1} \cdot \underline{V}_{\infty M}}{R_{M1} \, V_{\infty M}} \right) \right] \right\}^{-1} \qquad (3.4-13)$$

Then the initial velocity at the moon is

$$\underline{V}_{M1} = 1/2 \left(1 + \sqrt{X_M} \right) \underline{V}_{\infty M} - \frac{V_{\infty M}}{2R_{M1}} \left(1 - \sqrt{X_M} \right) \underline{R}_{M1} \qquad (3.4-14)$$

Equations (3.4-9) through (3.4-14) constitute a linear solution to the boundary value problem. They must be solved in a certain sequence to obtain zeroth-, first-, and second-order approximations (cf. Section 3.2 for a discussion of the steps involved). Equations (3.4-13) and (3.4-14) must be included in the sequence since the constants in (3.4-11) and (3.4-12) are functions of $\underline{R}_{M1}$ and $\underline{V}_{M1}$.

Combining (3.4-14) with the prescribed value of $\underline{R}_{M1}$ gives a complete set of initial conditions (note that they are inner variables and that to obtain dimensional values $\underline{R}_{M1}$ must be multiplied by μ as well as the appropriate dimensional length scale) for a trajectory satisfying, to zeroth order, all the conditions of the boundary value problem. The terminal state is given by (3.4-7) and (3.4-9). The prescribed entry radius is satisfied exactly because of (3.4-6), while the flight path angle and inclination differ by order μ from the prescribed values due to (3.4-8).

An alternative, nonlinear solution can also be obtained in a manner similar to that discussed in Subsection 3.2 for Earth-to-moon trajectories. The new Lambert problem is defined by the position vectors

$$r_o'(t_M) = \underline{r}_o(t_M) + \mu \, \delta \underline{r}(t_M) \tag{3.4-15}$$

$$\underline{r}_o'(t_e) = \underline{r}_o'(r_e, \gamma_e, i_e) \tag{3.4-16}$$

where

$$\delta \underline{r}(t_M) = \underline{\mathscr{L}}_M + \underline{Y}_M + \mu \, \underline{\zeta}_M \tag{3.4-17}$$

Equation (3.4-15) defines the fixed position vector for the modified Lambert problem and (3.4-16) represents the prescribed entry conditions. Solution of the new Lambert problem gives the final position, $\underline{r}_o'(t_e)$, and the initial and final velocities, $\underline{v}_o'(t_M)$ and $\underline{v}_o'(t_o)$. The excess velocity is

$$\underline{V}_{\infty M} = \underline{V}_M' + \mu \, \delta \underline{V}_\infty' \tag{3.4-18}$$

where

$$\underline{V}_M' = \underline{v}_o'(t_M) - \dot{\underline{p}}_M(t_M) \tag{3.4-19}$$

$$\underline{V}_\infty = - \underline{\delta}_M - \mu \, \underline{n}_M' \tag{3.4-20}$$

The initial velocity relative to the moon is still defined by (3.4-14). This solution requires the same sequence of steps as the nonlinear Earth-to-moon solution discussed in Subsection 3.2 except that the Lambert problems are of the modified rather than standard type.

For each of the zeroth-, first-, and second-order approximations the entry velocity is given by

$$\underline{v}(t_e) = \underline{v}_o'(t_e) \tag{3.4-21}$$

31

i.e., the entry velocity is the velocity of the modified Lambert solution. Since all of the Lambert solutions satisfy the entry constraints, the nonlinear solution satisfies these constraints to any order. Thus the nonlinear solution has the advantage that it satisfies the entry boundary conditions exactly rather than to zeroth order as the linear solution does. The nonlinear solution is shown in Figure 6.

The constants $\underline{Y}_M$, δ_M, $\underline{\zeta}_M$, and $\underline{\eta}_M$ are again fixed through each step. The function $\underline{\mathcal{X}}_M$, however, depends on $\underline{R}_{M1}$ and $\underline{V}_{M1}$ and must be evaluated for each approximation. In addition, because of (3.4-4), $\tau_M \neq 0$ and must be calculated with the other constants. This is expected since $\underline{V}_{M1}$ will not, in general, be normal to $\underline{R}_{M1}$, i.e., the initial position is not pericenter. The parameter τ_M is a measure of the time between t_1 and the time of pericenter passage. Formulas for calculating all of the constants are given in Subsection 3.8.
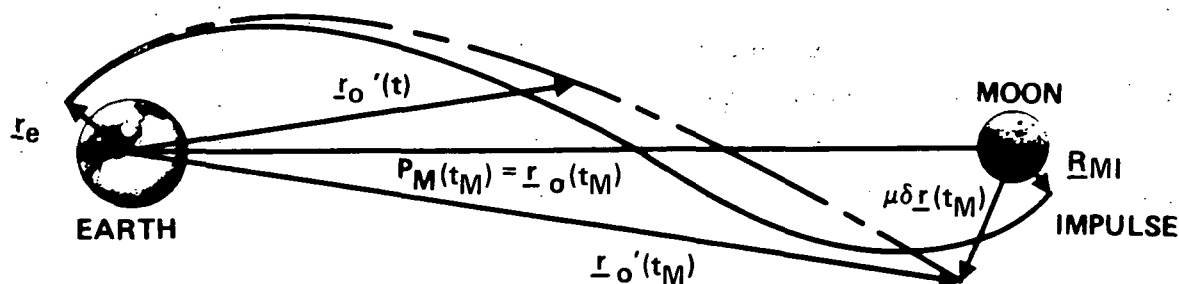
Figure 6. Nonlinear Version of One-Impulse Moon-to-Earth Solution

The initial velocity $\underline{V}_{M1}$ is the velocity after the impulse. The notation represents the velocity at t_1^+, i.e.,

$$\underline{V}_{M1} = \underline{V}_M(t_1^+) \tag{3.4-22}$$

If $\underline{V}_M(t_1^-)$ is the velocity before the impulse then the single impulse is given by

$$\Delta V = \underline{V}_M(t_1^+) - \underline{V}_M(t_1^-)$$

$$= \underline{V}_{M1} - \underline{V}_M(t_1^-) \tag{3.4-23}$$

3.5 TWO-IMPULSE MOON-TO-EARTH SOLUTION

The two-impulse moon-to-Earth problem is similar to the one-impulse problem discussed in the previous section except that the initial velocity is assumed to be known and does not give a trajectory satisfying the prescribed entry conditions. A second impulse is applied at some time prior to reaching the moon's sphere of influence resulting in a trans-Earth trajectory which does satisfy the entry conditions.

The boundary value problem is shown in Figure 7. The initial time, t_1, the initial position and velocity relative to the moon, $\underline{R}_{M1}$ and $\underline{V}_{M1}$, an initial impulse, I_1, along the current velocity vector at t_1, the time of the second impulse, t_2, and the entry time, t_e, radius, r_e, flight path angle, γ_e, and inclination, i_e, are all prescribed. The magnitude and direction of the second impulse are unknown and must be determined from the asymptotic solution.

The solution may or may not be derived from the fundamental solution. If the second impulse occurs well outside the moon's sphere of influence then the fundamental solution, derived from the matching process, should be used for the part of the solution between the first and second impulses. However, when the second impulse occurs near or inside the sphere of influence, Carlson (Reference 2) has shown numerically that a perturbed hyperbola is more accurate than the fundamental solution. His results have been verified theoretically by considering the order of magnitudes of all the error.
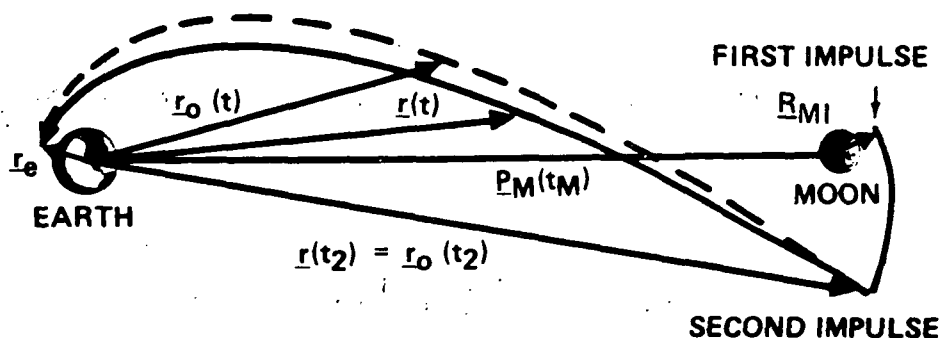
Figure 7. Two-Impulse Moon-to-Earth Solution

terms at various points out to and slightly beyond the sphere of influence (cf. Section B4. 3 of Volume 2).

The solution described here utilizes a perturbed hyperbola between the first and second impulses and a perturbed ellipse between the second impulse and Earth entry. The solution therefore is not a matched solution but simply two asymptotic solutions joined at the point of the second impulse.

The initial position and velocity (in inner variables) are

$$\underline{R}_M(S_1) \equiv \underline{R}_{M1} \tag{3.5-1}$$

$$\underline{V}_M(S_1^-) \equiv \underline{V}_{M1} \tag{3.5-2}$$

34

where S_1^- indicates the instant just prior to the first impulse which is defined as

$$\Delta \underline{V}_1 = I_1 \underline{V}_M(S_1^-) \qquad (3.5\text{-}3)$$

The position after the first impulse is still given by (3.5-1), but the velocity is now

$$\underline{V}_M(S_1^+) = (1 + I_1)\, \underline{V}_M(S_1^-) \qquad (3.5\text{-}4)$$

i.e., the post-impulse velocity is parallel to the initial velocity. The impulse I_1 must be chosen to make

$$V_{\infty M}^2 = V_M^2(S_1^+) - 2/R_M(S_1) \geq 0 \qquad (3.5\text{-}5)$$

i.e.,

$$I_1 \geq \left(\sqrt{2/R_M(S_1)}\right)/V_M(S_1^-) - 1 \qquad (3.5\text{-}6)$$

This is needed to guarantee a hyperbolic orbit after the impulse.

35

The post-impulse position and velocity uniquely define a zeroth-order hyperbolic trajectory about the moon. Position and velocity, R_{-Mo} and V_{-Mo}, as a function of the inner time S, can be determined from standard formulas such as (2.2-11). In addition the position and velocity can be used to determine the eccentricity and mean motion of the hyperbola as well as the initial eccentric anomaly $\overline{F}_1$ [cf. Carlson (Reference 2)], Volume 2, or Subsection 3.8]. Then the initial inner time is

$$S_1 = (\overline{e} \sinh \overline{F}_1 - \overline{F}_1)/\overline{n} \qquad (3.5-7)$$

and the inner time of the second impulse is

$$S_2 = S_1 + (t_2 - t_1)/\mu \qquad (3.5-8)$$

The position and velocity at t_2, including the perturbations due to the Earth, are

$$\underline{R}_M(S_2) = \underline{R}_{Mo}(S_2) + \mu^2 G_M \left[\underline{R}_{Mo}(S_2) \frac{S_2^2}{2} - \underline{V}_{Mo}(S_2) \frac{S_2^3}{3} \right]$$

$$+ \mu^3 \underline{A}_3 S_2^4 \qquad (3.5-9)$$

$$\underline{V}_M(S_2) = \underline{V}_{Mo}(S_2) + \mu^2 G_M \left[\underline{R}_{Mo}(S_2) S_2 - \underline{V}_{Mo}(S_2) \frac{S_2^2}{2} \right]$$

$$+ 4\mu^3 \underline{A}_3 S_2^3 \qquad (3.5-10)$$

where G_M and $\underline{A}_3$ are defined in Subsection 3.8. Transforming to Earth-centered coordinates using (2.2-1) and (2.2-2) gives

$$\underline{r}(t_2) = \underline{p}_M(t_2) + \mu \underline{R}_M(S_2) \qquad (3.5-11)$$

$$V(t_2^-) = \dot{p}_M (t_2) + \underline{V}_M (S_2) \qquad (3.5\text{-}12)$$

The solution between t_2 and t_e is given by (2.1-12), (2.1-13) and (2.1-14) with $t_o = t_e$ and $t = t_2$.

The zeroth-order solution is found from a modified Lambert problem with the initial position given by

$$\underline{r}_o(t_2) = \underline{r}(t_2) \qquad (3.5\text{-}13)$$

and the terminal position defined by

$$\underline{r}_o(t_e) = \underline{r}_o (r_e, \gamma_e, i_e) \qquad (3.5\text{-}14)$$

where (3.5-14) represents the prescribed entry conditions. Solution of the modified Lambert problem gives $\underline{r}_o (t_e)$, $\underline{r}_o (t)$ shown as the dashed line in Figure 7, and the zeroth-order velocities, $\underline{v}_o (t_2^+)$ and $\underline{v}_o (t_e)$.

As shown in Figure 7, the position perturbation at t_e can be made to vanish giving

$$\underline{r}_1(t_e) = \underline{r}_2 (t_e) = O \qquad (3.5\text{-}15)$$

so that

$$\underline{r}(t_e) = \underline{r}_o (t_e) \qquad (3.5\text{-}16)$$

The velocity perturbation

$$\delta \underline{v}(t_e) = \underline{v}_1 (t_e) + \mu \underline{v}_2 (t_e) \neq O \qquad (3.5\text{-}17)$$

does not vanish, so the entry velocity is

$$\underline{v}(t_e) = \underline{v}_o(t_e) + \mu \, \delta\underline{v}(t_e) \qquad (3.5\text{-}18)$$

By combining (3.5-10) and (3.5-11) with (2.1-12) through (2.1-14), the entry velocity perturbation and the velocity impulse at t_2 can be written

$$\delta\underline{v}(t_e) = -B(t_2, t_e)^{-1} \left[\underline{\Gamma}_{10}(t_2, t_e) + \mu \, \underline{\Gamma}_{20}(t_2, t_e) \right] \qquad (3.5\text{-}19)$$

$$\Delta V_2 = \underline{v}_o(t_2^+) - \underline{v}(t_2^-) + \mu \left[\underline{\Gamma}_{11}(t_2, t_e) + D(t_2, t_e) \, \delta\underline{v}(t_e) \right]$$

$$+ \mu^2 \, \underline{\Gamma}_{21}(t_2, t_e) \qquad (3.5\text{-}20)$$

where $\underline{\Gamma}_{10}$, $\underline{\Gamma}_{11}$, $\underline{\Gamma}_{20}$ and $\underline{\Gamma}_{21}$ are constants defined in Subsection 3.8. Equations (3.5-17) through (3.5-19) constitute a linear solution to the boundary value problem. Equation (3.5-18) gives the deviation from the prescribed entry conditions of γ_e and i_e $\left[r_e \text{ is satisfied due to } (3.5\text{-}14) \right]$ and (3.5-19) gives the velocity impulse which satisfies the entry conditions to zeroth order. Note that $\Delta\underline{V}_2$ is a function of t_2, of $\underline{R}_{M1}$, $\underline{V}_{M1}$, and I_1 (through $\underline{v}(t_2^-)$), of r_e, γ_e and i_e (through $\underline{v}_o(t_2^+)$), and the perturbations due to the moon and sun (through the Γ's). Therefore $\Delta\underline{V}_2$ is a function of all the boundary conditions.

An alternative, nonlinear solution can be obtained by solving a modified Lambert problem between the position vectors

$$\underline{r}_o'(t_2) = \underline{r}(t_2) - \mu \, \underline{\Gamma}_{10}(t_2, t_e) - \mu^2 \, \underline{\Gamma}_{20}(t_2, t_e) \qquad (3.5\text{-}21)$$

$$\underline{r}_o'(t_e) = \underline{r}_o'(r_e, \gamma_e, i_e) \qquad (3.5\text{-}22)$$

where $r_o'(t_2)$ is the fixed position vector and $r_o'(t_e)$ represents the prescribed boundary conditions. Solution of the new modified Lambert problem gives the velocities $v_o'(t_2^+)$ and $v_o'(t_e)$. The impulsive velocity becomes

$$\Delta V_2 = v_o'(t_2^+) - v(t_2^-) + \mu \, \Gamma_{11}(t_2, t_e) + \mu^2 \, \Gamma_{21}(t_2, t_e) \qquad (3.5\text{-}23)$$

and again, ΔV_2 is a function of all the boundary conditions.

The entry velocity is

$$v(t_e) = v_o'(t_e) \qquad (3.5\text{-}24)$$

and since $v_o(t_e)$ comes from a modified Lambert solution, the nonlinear solution satisfies the entry conditions exactly to any order. Therefore, just as in the one-impulse case, the nonlinear solution has the advantage of satisfying the boundary value problem exactly rather than to zeroth order as the linear solution does. The nonlinear solution is shown in Figure 8.
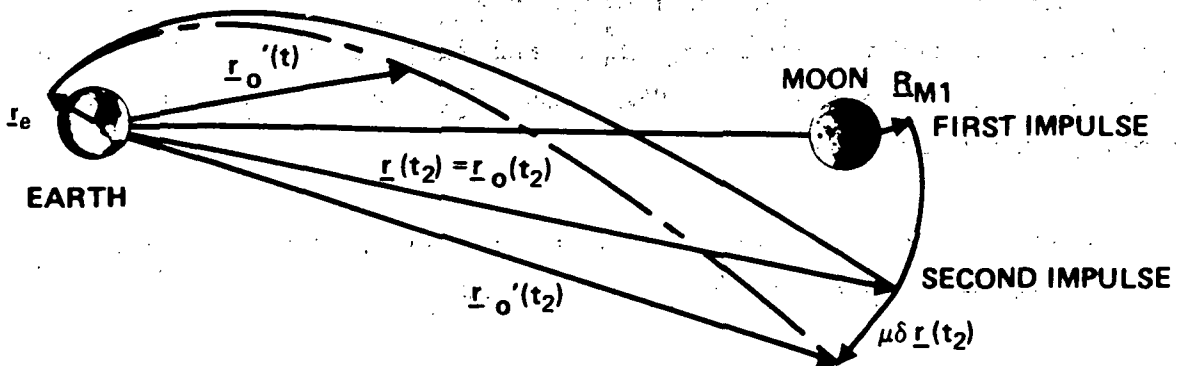
Figure 8. Nonlinear Version of Two-Impulse Moon-to-Earth Solution

39

3.6 INTERPLANETARY MIDCOURSE SOLUTION

The interplanetary midcourse solution is similar to the Earth-to-moon midcourse solution and therefore similar to the Earth-to-moon solution. The main difference is that this is an N-body solution where motion takes place in heliocentric rather than geocentric space. N may vary from three up to eleven, the latter being the entire solar system plus the particle. The target body (one of the nine planets) may also be the reference body. Letting T indicate the target body gives

$$k = T \tag{3.6-1}$$

$$\mu = \mu_T \tag{3.6-2}$$

The boundary value problem is shown in Figure 9. The initial time, t_o, the initial position relative to the sun, $\underline{r}(t_o)$, and the pericenter radius, $\overline{\rho}_T$, inclination, $\overline{i}_T$, and time, t_{pT}, at the target planet are all prescribed.
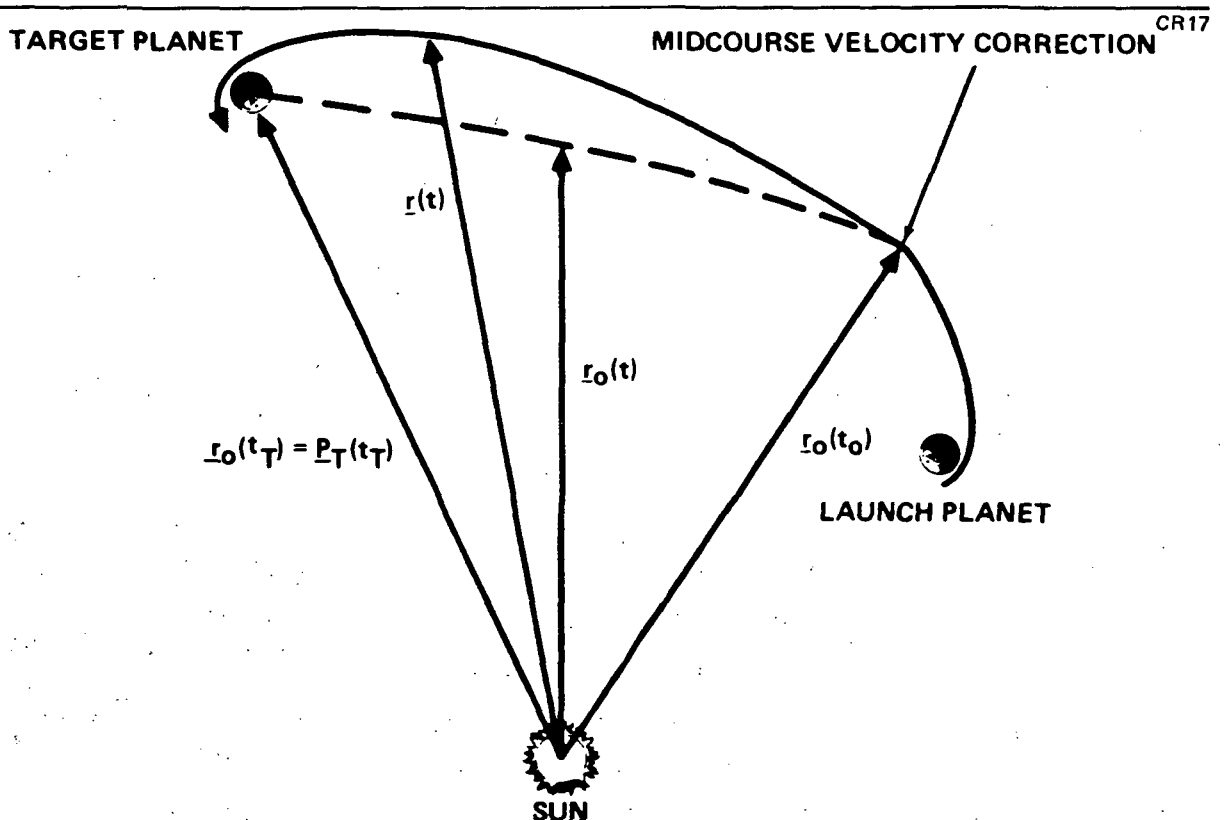
Figure 9. Interplanetary Midcourse Solution

The initial velocity, $\underline{v}(t_o)$, is unknown. An ephemeris giving positions of the N-2 planets in Cartesian coordinates relative to the sun is required to obtain the solution.

The solution is identical to the Earth-to-moon solution described in Subsection 3.2. That is, the initial velocity $\underline{v}(t_o)$ is found from the equations of Subsection 3.2 with M replaced by T and with μ equal to μ_T rather than μ_M.

The midcourse velocity correction is found from (3.3-1). Both the linear and nonlinear solutions are applicable to this problem although in actual practice the linear may be sufficient, as conditions favoring the nonlinear solution are not as likely to occur as they are in the Earth-to-moon solution.

3.7 INTERPLANETARY SOLUTION

The interplanetary solution is similar to the previous solution in that both apply to the general N-body problem. There is a fundamental difference between this solution and all the others in that the trajectory passes close to two perturbing bodies, one at the launch end of the trajectory and one at the target end. Letting L indicate the launch body and T the target body gives

$$k_{(1)} = L \tag{3.7-1}$$

$$k_{(2)} = T \tag{3.7-2}$$

The reference body may be either L or T, but to be consistent with the previous solution let

$$\mu = \mu_T \tag{3.7-3}$$

The interplanetary boundary value problem is shown in Figure 10. The pericenter radius, $\overline{\rho}_k$, inclination, $\overline{i}_k$, and time, t_{pk}, are prescribed at both the launch planet, $k = L$, and the target planet, $k = T$. The hyperbolic excess
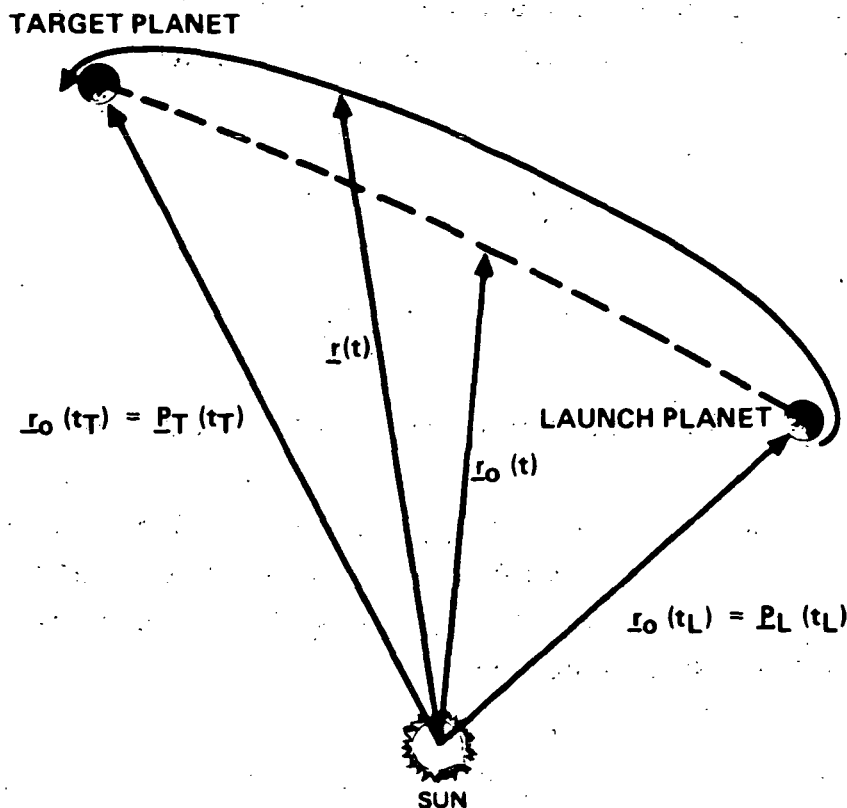
Figure 10. Interplanetary Solution

velocities relative to the sun as well as the pericenter positions and velocities relative to the respective bodies are unknown. The solution requires an ephemeris giving planetary positions relative to the sun.

From (2.2-3)

$$t_L = t_{pL} - \mu \tau_L \tag{3.7-4}$$

$$t_T = t_{pT} - \mu \tau_T \tag{3.7-5}$$

where, as in the Earth-to-moon solution, the τ's are arbitrary and can be set equal to zero without loss of generality.

From Figure 10 it can be seen that the zeroth-order ellipse, $\underline{r}_o(t)$, passes through the launch planet at $t = t_L$ and through the target planet at $t = t_T$, therefore

$$\underline{r}_o(t_L) = \underline{p}_L(t_L) \tag{3.7-6}$$

$$\underline{r}_o(t_T) = \underline{p}_T(t_T) \tag{3.7-7}$$

where $\underline{p}_L$ and $\underline{p}_T$ are the positions obtained from the ephemeris.

The two position vectors, $\underline{r}_o(t_L)$ and $\underline{r}_o(t_T)$, define a Lambert problem and the solution gives $\underline{r}_o(t)$, shown as the dashed line in Figure 10, and the initial and final zeroth-order velocities, $\underline{v}_o(t_L)$ and $\underline{v}_o(t_T)$. These velocities are used to define the relative velocities.

$$\underline{V}_L = \underline{v}_o(t_L) - \underline{\dot{p}}_L(t_L) \tag{3.7-8}$$

$$\underline{V}_T = \underline{v}_o(t_T) - \underline{\dot{p}}_T(t_T) \tag{3.7-9}$$

where $\underline{\dot{p}}_L$ and $\underline{\dot{p}}_T$ are velocities obtained from the ephemeris.

Now let the hyperbolic excess velocities be defined by

$$\underline{V}_{\infty L} = \underline{V}_L + \mu\, \delta\underline{V}_{\infty L} \tag{3.7-10}$$

$$\underline{V}_{\infty T} = \underline{V}_T + \mu\, \delta\underline{V}_{\infty T} \tag{3.7-11}$$

The perturbation terms in (3.7-10) and (3.7-11) are obtained from two fundamental solutions (Reference 12), one with k = L and one with k = T, which can be combined to give

$$\delta \underline{V}_{\infty L} = B(t_T, t_L)^{-1} \left\{ \underline{\mathscr{X}}_T + \underline{Y}_T + \mu \underline{\zeta}_T - A(t_T, t_L)(\underline{\mathscr{X}}_L + \underline{Y}_L + \mu \underline{\zeta}_L) \right\}$$

$$- \underline{\delta}_L - \mu \underline{\eta}_L \qquad\qquad (3.7-12)$$

$$\delta \underline{V}_{\infty T} = C(t_T, t_L)(\underline{\mathscr{X}}_L + \underline{Y}_L + \mu \underline{\zeta}_L) + \mu D(t_T, t_L)(\delta \underline{V}_{\infty L} + \underline{\delta}_L + \mu \underline{\eta}_L)$$

$$- \underline{\delta}_T - \mu \underline{\eta}_T \qquad\qquad (3.7-13)$$

The position and velocity at pericenter relative to either L or T are given by the inner variables

$$\underline{R}_{pk} = \frac{\bar{\rho}k}{\bar{a}_k \bar{e}_k} \underline{L}_k \qquad\qquad (3.7-14)$$

$$\underline{V}_{pk} = \frac{1}{\bar{a}_k \bar{e}_k} \left(\frac{1 + \bar{e}_k}{\bar{\rho}k} \right)^{1/2} \frac{\partial \underline{L}k}{\partial \bar{\omega}k} \qquad\qquad (3.7-15)$$

Equations (3.7-10) through (3.7-15) constitute a linear solution of the boundary value problem. Since $\underline{V}_{\infty L}$ and $\underline{V}_{\infty T}$ enter the right-hand sides of (3.7-12) and (3.7-13) through $\underline{\mathscr{X}}_L$ and $\underline{\mathscr{X}}_T$ the relations are not explicit but must be solved in a sequence using the zeroth-, first-, and second-order terms successively. The zeroth-order approximation is obtained by putting $\mu = 0$ in (3.7-10) and (3.7-11). The first-order approximation is obtained by putting $\mu = 0$ in (3.7-12) and (3.7-13) (but not μ_L or μ_T) and using the zeroth-order $\underline{V}_\infty$'s in the right-hand sides of these equations. The second-order approximation is obtained by using the first-order $\underline{V}_\infty$'s in the right-hand sides of (3.7-12) and (3.7-13). Finally the values of $\underline{V}_{\infty L}$ and $\underline{V}_{\infty T}$, along with the prescribed boundary conditions at each end, are used to evaluate (3.7-14) and (3.7-15) for k = L and k = T giving the initial and final positions

and velocities relative to the launch and target bodies, respectively. All the additional equations needed to evaluate the complete solution are given in Subsection 3.8.

The linear solution does not show any explicit dependence on the time $t = t_o$ which appears in the fundamental solution. The solution is a function of t_o however since the constants are evaluated either between t_L and t_o or between t_o and t_T (cf. Subsection 3.8). This requires knowledge of not only $\underline{r}_o(t)$ but also $\underline{r}_1(t)$ and $\underline{v}_1(t)$. The time t_o itself is arbitrary to a certain extent, and a logical choice would be

$$t_o = (t_L + t_T)/2$$

The value of $\underline{r}_o(t_o)$ can then be obtained from the original Lambert solution for $\underline{r}_o(t)$ and the values of $\underline{r}_1(t_o)$ and $\underline{v}_1(t_o)$ can be obtained from the fundamental solution with either $k = L$ or $k = T$ and $\mu = 0$.

If $\underline{r}_1(t_o)$ is very large then the deviation between the zeroth- and first-order solutions may introduce large errors. These errors can be reduced by defining a modified linear solution as follows:

The three position vectors

$$\underline{r}'_o(t_L) = \underline{p}_L(t_L) \tag{3.7-16}$$

$$\underline{r}'_o(t_o) = \underline{r}''_o(t_o) = \underline{r}_o(t_o) + \mu\,\underline{r}_1(t_o) \tag{3.7-17}$$

$$\underline{r}''_o(t_T) = \underline{p}_T(t_T) \tag{3.7-18}$$

define the new Lambert problems. The solution of the first Lambert problem gives $\underline{r}'_o(t)$, shown as the dashed line in Figure 11, and the two zeroth-order velocities, $\underline{v}'_o(t_L)$ and $\underline{v}'_o(t_o)$. The solution of the second Lambert problem gives $\underline{r}''_o(t)$, shown as the dotted line in Figure 11, and the two zeroth-order velocities, $\underline{v}''_o(t_o)$ and $\underline{v}''_o(t_T)$.

TARGET PLANET

$\mu \underline{r}_1(t_o)$

$\underline{r}_o'''(t)$

$\underline{r}_o(t_o)$

$\underline{r}_o'(t_o) = \underline{r}_o'''(t_o)$

$\underline{P}_T(t_T)$

LAUNCH PLANET

$\underline{r}_o'(t)$

$\underline{P}_L(t_L)$

SUN
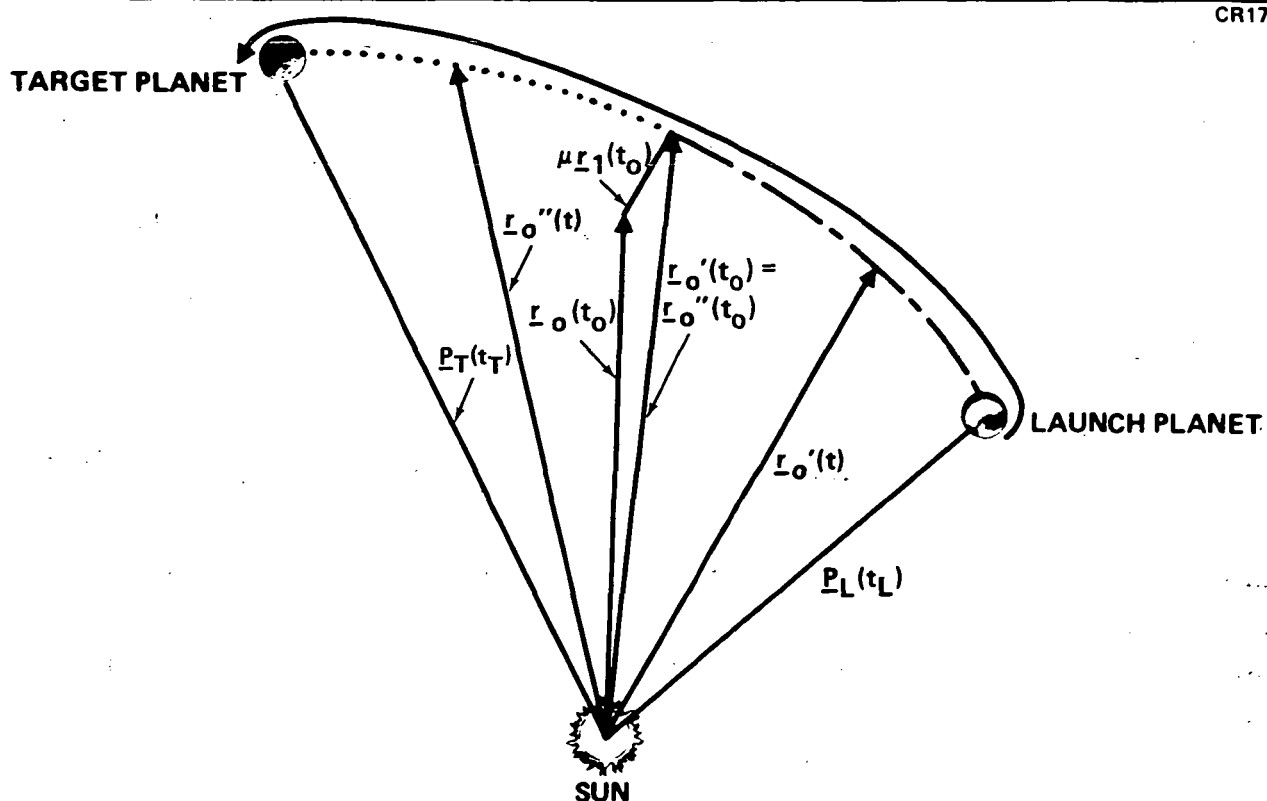
Figure 11. Modified Linear Version of Interplanetary Solution

The relative velocities are defined by

$$\underline{V}_L' = \underline{v}_o'(t_L) - \underline{\dot{p}}_L(t_L) \tag{3.7-19}$$

$$\underline{V}_T'' = \underline{v}_o''(t_T) - \underline{p}_T(t_T) \tag{3.7-20}$$

while a new intermediate velocity is defined by

$$\underline{v}_1'(t_o) = \left[\underline{v}_o''(t_o) - \underline{v}_o'(t_o) \right] / \mu \tag{3.7-21}$$

Now let the excess velocities be defined by

$$\underline{V}_{\infty L} = \underline{V}_L' + \mu \, \delta \underline{V}_{\infty L}' \tag{3.7-22}$$

$$\underline{V}_{\infty T} = \underline{V}_T' + \mu \, \delta \underline{V}_{\infty T}' \tag{3.7-23}$$

46

where the perturbation terms are obtained from the fundamental solution as

$$\delta \underline{V}'_{\infty L} = \tilde{B}\,(t_T, \ t_L)^{-1} \left| \underline{\mathscr{X}}_T{}'' + \underline{Y}_T{}'' + \mu\,\underline{\zeta}_T{}'' - \tilde{A}\,(t_T, \ t_L)\,(\underline{\mathscr{X}}_L{}' + \underline{Y}_L{}' + \mu\,\underline{\zeta}_L{}') \right.$$

$$\left. + B''\,(t_T, \ t_o)\,\underline{v}'_1(t_o) \right| - \underline{\delta}'_L - \mu\,\underline{\eta}'_L \qquad (3.7\text{-}24)$$

$$\delta \underline{V}'_{\infty T} = \tilde{C}\,(t_T, \ t_L)\,(\underline{\mathscr{X}}_L{}' + \underline{Y}_L{}' + \mu\,\underline{\zeta}_L{}') + \tilde{D}\,(t_T, \ t_L)\,(\delta \underline{V}'_{\infty L} + \underline{\delta}'_L + \mu\,\underline{\eta}'_L)$$

$$- D''\,(t_T, \ t_o)\,\underline{v}'_1(t_o) - \underline{\delta}''_T - \mu\,\underline{\eta}''_T \qquad (3.7\text{-}25)$$

In (3.7-24) and (3.7-25) the superscripts prime (') and double prime (") indicate that the parameter (constant, matrix, function) is evaluated along either $\underline{r}'_o$ or $\underline{r}''_o$ respectively. The superscript tilde (~) indicates a special partial derivative matrix defined by

$$\tilde{\Phi}\,(t_T, \ t_L) = \Phi''\,(t_T, \ t_o)\,\Phi'\,(t_o, \ t_L) \qquad (3.7\text{-}26)$$

so that

$$\tilde{A}(t_T, \ t_L) = A''\,(t_T, \ t_o)\,A'\,(t_o, \ t_L) + B''\,(t_T, \ t_o)\,C'\,(t_o, \ t_L) \qquad (3.2\text{-}27)$$

$$\tilde{B}(t_T, \ t_L) = A''\,(t_T, \ t_o)\,B'\,(t_o, \ t_L) + B''\,(t_T, \ t_o)\,D'\,(t_o, \ t_L) \qquad (3.7\text{-}28)$$

$$\tilde{C}(t_T, \ t_L) = C''\,(t_T, \ t_o)\,A'\,(t_o, \ t_L) + D''\,(t_T, \ t_o)\,C'\,(t_o, \ t_L) \qquad (3.7\text{-}29)$$

$$\tilde{D}(t_T, \ t_L) = C''\,(t_T, \ t_o)\,B'\,(t_o, t_L) + D''\,(t_T, \ t_o)\,D'\,(t_o\ t_L) \qquad (3.7\text{-}30)$$

The special notation is required because the two zeroth-order solutions, $\underline{r}'_o$ and $\underline{r}''_o$, are not continuous in velocity at $t = t_o$. Therefore, the transition matrix has discontinuities at $t = t_o$. These discontinuities are removed by (3.7-26).

Equations (3.7-22) through (3.7-30) along with (3.7-14) and (3.7-15) constitute a modified linear solution to the boundary value problem. It must be evaluated using the same sequence of steps as the linear solution and can only be started after $\underline{r}_1(t_o)$ is found from the linear solution. It thus requires more computation time, but forcing the Lambert solutions closer to the actual trajectory at $t-t_o$ reduces the size of the perturbation terms with a resultant increase in accuracy (cf. the section on numerical results).

The nonlinear interplanetary solution is obtained from the solutions of a sequence of Lambert problems defined by the position vectors

$$\underline{r}_o''' (t_L) = \underline{p}_L (t_L) + \mu \, \underline{\delta r} (t_L) \tag{3.7-31}$$

$$\underline{r}_o''' (t_T) = \underline{p}_T (t_T) + \mu \, \underline{\delta r} (t_T) \tag{3.7-32}$$

where

$$\underline{\delta r}(t_L) = \underline{\mathscr{L}}_L + \underline{\gamma}_L + \bar{\mu} \, \underline{\zeta}_L \tag{3.7-33}$$

$$\underline{\delta r}(t_T) = \underline{\mathscr{L}}_T + \underline{\gamma}_T + \mu \, \underline{\zeta}_T \tag{3.7-34}$$

Solution of the Lambert problems gives the initial and final velocities, $\underline{V}_o''' (t_L)$ and $\underline{V}_o''' (t_T)$. The excess velocities become

$$\underline{V}_{\infty L} = \underline{V}_L''' + \mu \, \underline{V}_{\infty L}''' \tag{3.7-35}$$

$$\underline{V}_{\infty T} = \underline{V}_T''' + \mu \, \underline{V}_{\infty T}''' \tag{3.7-36}$$

where

$$\underline{V}_L''' = \underline{\dot{v}}_o''' (t_L) - \underline{\dot{p}}_L (t_L) \tag{3.7-37}$$

$$\underline{V}_T''' = \underline{v}_o''' (t_T) - \underline{\dot{p}}_T (t_T) \tag{3.7-38}$$

and

$$\delta \underline{V}'''_{\infty L} = -\underline{\delta}_L - \mu \, \underline{\eta}_L \qquad (3.7-39)$$

$$\delta \underline{V}'''_{\infty T} = -\underline{\delta}_T - \mu \, \underline{\eta}_T \qquad (3.7-40)$$

This solution also requires a sequence of steps. The zeroth-order solution, identical with the zeroth-order linear solution, is obtained by putting $\mu = 0$ in (3.7-31), (3.7-32), (3.7-35), and (3.7-36). The first-order approximation is obtained by putting $\mu = 0$ in (3.7-33), (3.7-34), (3.7-39), and (3.7-40) and using the first order $\underline{V}_\infty$'s in the right-hand sides of (3.7-33) and (3.7-34). The second-order approximation is obtained by using the first-order $\underline{V}_\infty$'s in (3.7-33) and (3.7-34). The nonlinear solution is shown in Figure 12.

CR17
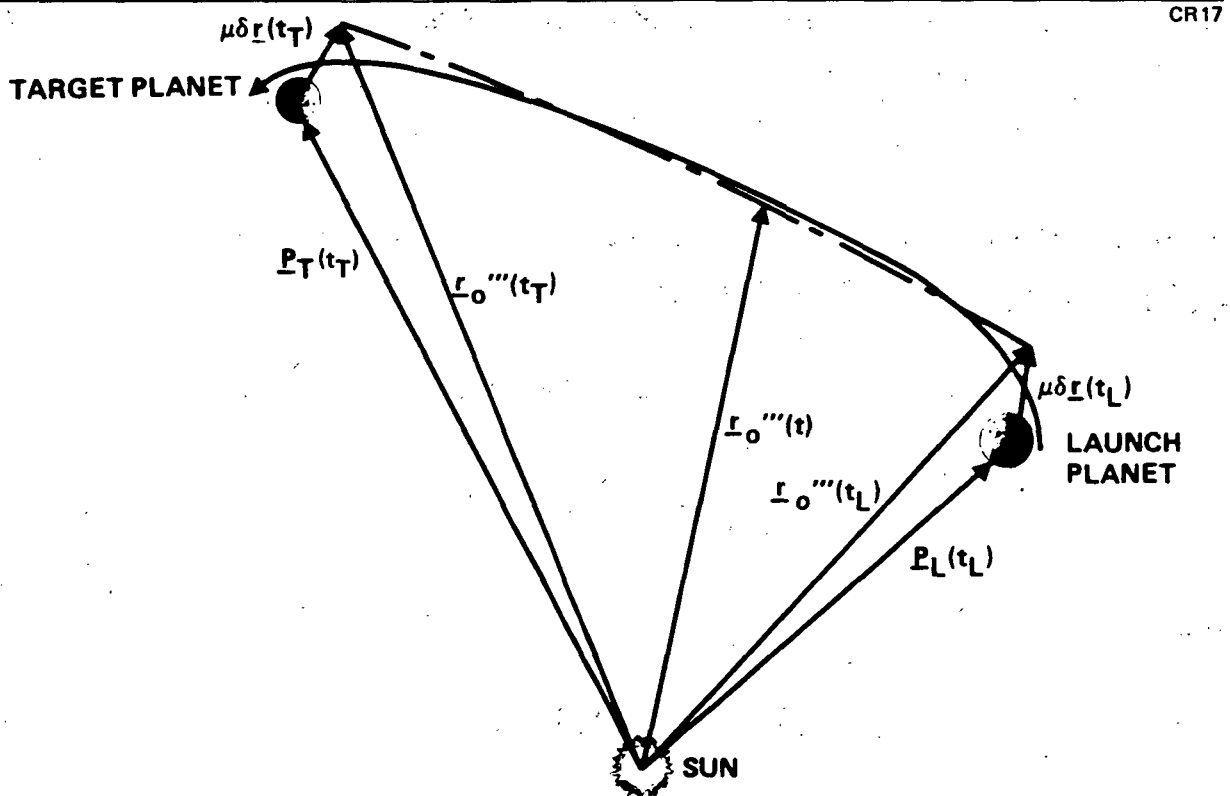
Figure 12. Nonlinear Version of Interplanetary Solution

49

It is tempting to define a modified nonlinear solution by replacing (3.7-33) and (3.7-34) with

$$\delta \underline{r}(t_L) = \underline{\mathscr{L}}'_L + \underline{Y}'_L + \mu \underline{\zeta}'_i \qquad (3.7\text{-}41)$$

$$\delta \underline{r}(t_T) = \underline{\mathscr{L}}''_T + \underline{Y}''_T + \mu \underline{\zeta}''_T + B''(t_T, t_o) \underline{v}'_1(t_o) \qquad (3.7\text{-}42)$$

The theoretical basis for making such a substitution is questionable since the matrix $\tilde{\Phi}(t_T, t_L)$, defined by (3.7-26), is not a true transition matrix. The nonlinear solution essentially replaces the transition matrix by a new Lambert solution to account for nonlinear effects in the partial derivatives. The modified nonlinear solution therefore involves the replacement of a pseudo-transition matrix with a Lambert problem and may not offer any improvement over the modified linear solution.

All the functions appearing in this section are defined by formulas which appear in the next section.

3.8 FORMULAS FOR THE BOUNDARY VALUE SOLUTIONS

Each of the preceding solutions requires at least one zeroth-order ellipse which is found as the solution of either a standard or a modified Lambert problem. Except in the two-impulse moon-to-Earth solution, the zeroth-order velocity at $t = t_k$ is used to define a relative velocity

$$\underline{V}_k = \underline{v}_o(t_k) - \underline{\dot{p}}_k(t_k) \qquad (3.8\text{-}1)$$

The relative velocity becomes the zeroth-order approximation to the hyperbolic excess velocity, i.e.,

$$\underline{V}_{\infty k} = \underline{V}_k + O(\mu) \qquad (3.8\text{-}2)$$

Thus in each of the solutions requiring knowledge of the excess velocity, a zeroth-order approximation can be obtained from the Lambert solution. The previous sections showed how the zeroth-order approximation becomes the starting point for generating successively higher-order approximations to $\underline{V}_{\infty k}$. The only steps left are to show how $\underline{V}_{\infty k}$ and the prescribed boundary conditions are used to generate the various parameters appearing in the boundary value solutions. The solutions of Subsections 3.2, 3.3, 3.6, and 3.7 all use the same formulas and these will be given first. The solution of Subsection 3.4 requires a few special formulas to make it fit with the other solutions. Finally the solution of Subsection 3.5 will be considered separately.

First consider the case where prescribed values of pericenter radius, $\overline{\rho}_k$, and inclination, $\overline{i}_k$, must be combined with $\underline{V}_{\infty k}$ to determine the inner hyperbola. The Cartesian components of $\underline{V}_{\infty k}$ are given by the vector notation

$$\underline{V}_{\infty k} = (\overline{U}_k, \overline{V}_k, \overline{W}_k) \tag{3.8-3}$$

where the bars indicate inner variables. In addition to the prescribed inclination $\overline{i}_k$, the elements of the hyperbola are (cf. Section B2 of Volume 2)

$$\overline{a}_k = V_{\infty k}^{-2} \tag{3.8-4}$$

$$\overline{e}_k = 1 + \overline{\rho}_k \underline{V}_{\infty k}^2 \tag{3.8-5}$$

$$\cos \overline{\Omega}_k = \frac{\text{ctn } \overline{i}_k}{(\overline{U}_k^2 + \overline{V}_k^2)} \left\{ \overline{V}_k \overline{W}_k \mp \overline{U}_k \left[(\overline{U}_k^2 + \overline{V}_k^2) \tan^2 \overline{i}_k - \overline{W}_k^2 \right]^{1/2} \right\}$$

$$\tag{3.8-6}$$

$$\sin \overline{\Omega}_k = - \frac{\operatorname{ctn} \overline{i}_k}{(\overline{U}_k^2 + \overline{V}_k^2)} \left\{ \overline{U}_k \overline{W}_k \pm \overline{V}_k \left[(\overline{U}_k^2 + \overline{V}_k^2) \tan^2 \overline{i}_k - \overline{W}_k^2 \right]^{1/2} \right\}$$

$$(3.8-7)$$

$$\sin \overline{\omega}_k = - \frac{\overline{a}_k^{1/2}}{\overline{e}_k} \left[(\overline{e}_k^2 - 1)^{1/2} \overline{U}_k' + Q_k \overline{V}_k' \right] \qquad (3.8-8)$$

$$\cos \overline{\omega}_k = \frac{\overline{a}_k^{1/2}}{\overline{e}_k} \left[(\overline{e}_k^2 - 1)^{1/2} \overline{V}_k' - Q_k \overline{U}_k' \right] \qquad (3.8-9)$$

where

$$\overline{U}_k' = \overline{U}_k \cos \overline{\Omega}_k + \overline{V}_k \sin \overline{\Omega}_k \qquad (3.8-10)$$

$$\overline{V}_k' = \frac{\overline{V}_k \cos \overline{\Omega}_k - \overline{U}_k \cos \overline{\Omega}_k}{\cos \overline{i}_k} \qquad (3.8-11)$$

$$= \frac{\overline{W}_k}{\sin \overline{i}_k} \qquad (3.8-12)$$

and

$$Q_k = \pm 1 \qquad (3.8-13)$$

The elements $\bar{a}_k$, $\bar{e}_k$, $\bar{\Omega}_k$ and $\bar{\omega}_k$ are the semimajor axis, eccentricity, argument of ascending node, and argument of pericenter, respectively. In (3.8-6) and (3.8-7) the upper sign is used if the approach to or departure from the $k\underline{\text{th}}$ body is to be over the body, and the lower sign is to be used if the approach or departure is under the body. In (3.2-12) the upper sign is used for departure from the $k\underline{\text{th}}$ body, and the lower sign for approach.

Additional constants which are used are derived in Sections A12 and B1 of Volume 2. They are:

$$\bar{n}_k = V_{\infty k}^3 \tag{3.8-14}$$

$$\bar{A}_k = \bar{a}_k \bar{e}_k (\cos \bar{\omega}_k \cos \bar{\Omega}_k - \sin \bar{\omega}_k \sin \bar{\Omega}_k \cos \bar{i}_k) \tag{3.8-15}$$

$$\bar{B}_k = \bar{a}_k \bar{e}_k (\cos \bar{\omega}_k \sin \bar{\Omega}_k + \sin \bar{\omega}_k \cos \bar{\Omega}_k \cos \bar{i}_k) \tag{3.8-16}$$

$$\bar{C}_k = \bar{a}_k \bar{e}_k \sin \bar{\omega}_k \sin \bar{i}_k \tag{3.8-17}$$

$$\underline{L}_k = (\bar{A}_k, \bar{B}_k, \bar{C}_k) \tag{3.8-18}$$

$$\underline{A}_{ko} = \underline{V}_{\infty k} \tag{3.8-19}$$

$$\underline{B}_{ko} = Q_k \underline{V}_{\infty k} / \bar{n}_k \tag{3.8-20}$$

$$\underline{C}_{ko} = Q_k \log (2 \bar{n}_k / \bar{e}_k) \underline{V}_{\infty k} / \bar{n}_k + \underline{L}_k \tag{3.8-21}$$

$$\underline{A}_{k2} = G_k \underline{A}_{ko} / 6 \tag{3.8-22}$$

$$\underline{B}_{k2} = G_k \underline{B}_{ko} / 2 \tag{3.8-23}$$

$$\overline{C}_{k2} = \left[G(\underline{A}_{ko}) \, \underline{A}_{k2} + G_k \, \underline{C}_{ko} - 3 \, \underline{B}_{k2} \right] / 2 \qquad (3.8\text{-}24)$$

$$\underline{A}^*_{k2} = M_k^2 \Bigg\{ \mu_k \, Q_k \, \underline{R}_{k2} \, (Q_k/\mu_k)$$

$$- \mu_k^{-2} \left[\underline{A}_{k2} - \mu_k \, Q_k \, \underline{B}_{k2} \, \log \mu_k + \mu_k \, Q_k \, \underline{C}_{k2} \right] \Bigg\}$$

$$(3.8\text{-}25)$$

The matrix $G(\underline{A}_{ko})$ is found from (2.1-8) with $\underline{x} = \underline{A}_{ko}$. The matrix G_k is defined as

$$G_k = G \, (\underline{p}_k \, (t_k)) \qquad (3.2\text{-}26)$$

The vector $\underline{R}_{k2} \, (Q_k/\mu_k)$ is found from (2.2-13) with $S_k = Q_k/\mu_k$. It must be determined by Gaussian quadrature or some other numerical means. An approximate value of $\underline{A}^*_{k2}$ can be found from

$$\underline{A}^*_{k2} = M_k^2 \left(\underline{D}_{k2} \, \log^2 \mu_k - \underline{E}_{k2} \, \log \mu_k \right) \qquad (3.2\text{-}27)$$

where

$$\underline{D}_{k2} = \left[G(\underline{A}_{ko}) \, \underline{B}_{k2} + \underline{H}(\underline{A}_{ko}) \, \underline{B}_{ko} \, \underline{A}_{k2} + G_k \, \underline{D}_{ko} \right] / 2 \qquad (3.2\text{-}28)$$

$$\underline{E}_{k2} = \left[G(\underline{A}_{ko}) \, \underline{C}_{k2} + \underline{H}(\underline{A}_{ko}) \, \underline{C}_{ko} \, \underline{A}_{k2} + G_k \, \underline{E}_{ko} - 2 \, \underline{D}_{k2} \right]$$

$$(3.2\text{-}29)$$

The tensor $\underline{H}(\underline{A}_{ko})$ is found from (2.1-9) with $\underline{x} = \underline{A}_{ko}$.

Formulas (3.8-4) through (3.8-13) give the constants which completely define the inner hyperbola R_{ko}. Formulas (3.8-14) - (3.8-21) are used to determine the behavior of R_{ko} in the overlap domain where S_k is large. The behavior of the perturbation, R_{k2}, when S_k is large can be found from (3.8-22) through (3.8-29). The key formulas are those for L_k and A_{k2}^* since they appear in (2.3-5) and eventually in the fundamental solution.

In the one-impulse moon-to-Earth solution the boundary conditions are not given as prescribed pericenter radius and inclination but rather as a pre-scribed initial time and position. The initial position R_{M1}, combined with $V_{\infty M}$ in (3.4-14), gives the initial velocity V_{M1}. The angular momentum magnitude, $\bar{\ell}_M$, is given by the relation

$$\bar{\ell}_M = \frac{R_{M1} \, V_{\infty M}}{2} \left(1 + \sqrt{X_M}\right) \sin\left[\cos^{-1}\left(\frac{R_{M1} \cdot V_{\infty M}}{R_{M1} \, V_{\infty M}}\right)\right] \tag{3.8-30}$$

The inclination is then defined by

$$\cos \bar{i}_M = (e_3 \cdot R_{M1} \times V_{M1}) / \bar{\ell}_M \tag{3.8-31}$$

where $\bar{e}_3$ is the unit vector in the z direction and x the vector cross product. The pericenter radius is obtained from

$$\bar{\rho}_M = \left[\left(1 + V_{\infty M}^2 \, \bar{\ell}_M^2\right)^{1/2} - 1\right] / V_{\infty M}^2 \tag{3.8-32}$$

Thus in the one-impulse solution (3.8-31) and (3.8-32) give the unknown $\bar{i}_M$ and $\bar{\rho}_M$ in terms of $V_{\infty M}$ and the boundary conditions. These two equations, as well as (3.8-30) must be added to the previous set of equations, (3.8-4) to (3.8-29), in order to define the inner hyperbola.

The time τ_k, which can be arbitrarily set to zero in the solutions of Subsections 3.2, 3.3, 3.6, and 3.7, has a fixed value in the one-impulse solution. The eccentric anomaly along the inner hyperbola at $t - t_1$ is found from

$$\cosh \overline{F}_1 = (\overline{a}_M + R_{M1}) / (\overline{a}_M \overline{e}_M) \qquad (3.8\text{-}33)$$

$$\sinh \overline{F}_1 = (\underline{V}_{M1} \cdot \underline{R}_{M1}) / (\overline{e}_M \overline{a}_M^{1/2}) \qquad (3.8\text{-}34)$$

Kepler's equation then gives τ_M as

$$\tau_M = (\overline{F}_1 - \overline{e}_M \sinh \overline{F}_1) / \overline{n}_M \qquad (3.8\text{-}35)$$

i.e., τ_M is the negative of the inner time from pericenter.

The expressions presented up to this point all pertain to the inner hyperbola about the $k^{\underline{th}}$ body. Another set of formulas defines all of the parameters related to the outer solution. Like the inner formulas they involve the matrix G defined by (2.1-8) and the tensor $\underline{H}$ defined by (2.1-2), as well as the vector function $\underline{f}$ defined by (2-2). These formulas, in order of solution, are

$$\underline{p}_k^* = M_k \, \underline{f} \, (\underline{p}_k \, (t_k))$$

$$+ \sum_{\substack{i=1 \\ i \neq k}}^{N-2} M_i \left[\underline{f} \, (\underline{p}_k \, (t_k) - \underline{p}_i \, (t_k)) + \underline{f} \, (\underline{p}_i \, (t_k)) \right] \qquad (3.8\text{-}36)$$

$$\underline{p}_k^{**} = M_k \, G_k \, \underline{\dot{p}}_k \, (t_k)$$

$$+ \sum_{\substack{i=1 \\ i \neq k}}^{N-2} M_i \left[G \left(\underline{p}_k (t_k) - \underline{p}_i (t_k) \right) \left(\underline{\dot{p}}_k (t_k) - \underline{\dot{p}}_i (t_k) \right) + G \left(\underline{p}_i (t_k) \right) \underline{\dot{p}}_i (t_k) \right]$$

$$(3.8-37)$$

$$\underline{H}_k = \underline{H} \left(\underline{p}_k (t_k) \right) \qquad (3.8-38)$$

$$\underline{\beta}_{1k} = Q_k \, M_k \, \underline{f} \, (\underline{V}_k) \qquad (3.8-39)$$

$$\underline{\beta}_{2k} = -\mu_k \, Q_k \, G \, (\underline{V}_k) \, \underline{p}_k^* / 2 \qquad (3.8-40)$$

$$\underline{\beta}_{3k} = Q_k \, M_k \, G(\underline{V}_k) \left[G_k \, \underline{V}_k - \mu \underline{p}_k^{**} \right] / 6 \qquad (3.8-41)$$

$$\underline{\beta}_{4k} = Q_k \, M_k \, G_k \, \underline{f} \, (\underline{V}_k) \, / 6 \qquad (3.8-42)$$

$$\underline{K}_{10k} (t_k, \, t_o) = \int_{t_o}^{t_k} \left[B \, (t_k, \tau) \, \underline{F}_1 \, (\tau) + \frac{\underline{\beta}_{1k}}{(\tau - t_k)} \right] d\tau \qquad (3.8-43)$$

$$\underline{K}_{11k} (t_k, \, t_o) = \int_{t_o}^{t_k} \left[D \, (t_k, \tau) \, \underline{F}_1 \, (\tau) - \frac{\underline{\beta}_{1k}}{(\tau - t_k)^2} - \frac{\underline{\beta}_{2k}}{(\tau - t_k)} \right] d\tau$$

$$(3.8-44)$$

$$\Gamma_k = \log\left[Q_k \left(t_o - t_k\right)\right] \tag{3.8-45}$$

$$\underline{a}_{1k} = -\underline{\beta}_{1k} \tag{3.8-46}$$

$$\underline{b}_{1k} = \underline{\beta}_{1k}\left(\Gamma_k - 1\right) + A\left(t_k, t_o\right)\underline{r}_1\left(t_o\right)$$
$$B\left(t_k, t_o\right)\underline{v}_1\left(t_o\right) + \underline{K}_{10k}\left(t_k, t_o\right) \tag{3.8-47}$$

$$\underline{c}_{1k} = \underline{\beta}_{2k}/\mu \tag{3.8-48}$$

$$\underline{d}_{1k} = \underline{\beta}_{1k}\left(t_o - t_k\right)^{-1} + C\left(t_k, t_o\right)\underline{r}_1\left(t_o\right)$$
$$+ D\left(t_k, t_o\right)\underline{v}_1\left(t_o\right) + \underline{K}_{11k}\left(t_k, t_o\right) \tag{3.8-49}$$

$$\underline{e}_{1k} = -\underline{\beta}_{2k}\left(\Gamma_k + 1\right)/\mu \tag{3.8-50}$$

$$\underline{f}_{1k} = -3\,\underline{\beta}_{4k} \tag{3.8-51}$$

$$\underline{g}_{1k} = \underline{\beta}_{3k}/2 + 3\underline{\beta}_{4k}\left(\Gamma_k + 1/2\right) + \underline{p}_k^*/2 + 1/2\,G_k\left[\underline{b}_{1k} - \underline{\beta}_{1k}\left(\Gamma_k - 1\right)\right] \tag{3.8-52}$$

$$G_k^* = M_k\,Q_k\,G(\underline{V}_k) \tag{3.8-53}$$

58

$$H_k^* = \frac{M_k Q_k}{2} \left[\frac{1}{3} \underline{H}(\underline{V}_k) (G_k \underline{V}_k - \mu \underline{p}_k^{**}) \right] \qquad (3.8\text{-}54)$$

$$J_k^* = \frac{M_k Q_k}{2} \underline{H}(\underline{V}_k) \underline{p}_k^* \qquad (3.8\text{-}55)$$

$$\underline{\psi}_{1k} = G_k^* \underline{a}_{1k} \qquad (3.8\text{-}56)$$

$$\underline{\psi}_{2k} = G_k^* \underline{b}_{1k} \qquad (3.8\text{-}57)$$

$$\underline{\psi}_{3k} = \mu (G_k^* \underline{c}_{1k} - J_k^* \underline{a}_{1k}) \qquad (3.8\text{-}58)$$

$$\underline{\psi}_{4k} = G_k^* \underline{d}_{1k} + \mu (G_k^* \underline{e}_{1k} - J_k^* \underline{b}_{1k}) \qquad (3.8\text{-}59)$$

$$\underline{\psi}_{5k} = G_k^* \underline{f}_{1k} + H_k^* \underline{a}_{1k} - \mu^2 J_k^* \underline{c}_{1k} \qquad (3.8\text{-}60)$$

$$\underline{\psi}_{6k} = G_k^* \underline{g}_{1k} + H_k^* \underline{b}_{1k} - \mu J_k^* (\underline{d}_{1k} + \mu \underline{e}_{1k}) \qquad (3.8\text{-}61)$$

$$\underline{\psi}_{7k} = G_k G_k^* \underline{a}_{1k} / 6 \qquad (3.8\text{-}62)$$

$$\underline{\psi}_{8k} = G_k G_k^* \underline{b}_{1k} / 6 \qquad (3.8\text{-}63)$$

$$\underline{K}_{20k} (t_k, t_o) = \int_{t_o}^{t_k} \left[B(t_k, \tau) \, \underline{F}_2(\tau) + \underline{\psi}_{1k} \frac{\log Q_k (\tau - t_k)}{(\tau - t_k)^2} \right.$$

$$+ \underline{\psi}_{2k} \frac{1}{(\tau - t_k)^2} + \underline{\psi}_{3k} \frac{\log Q_k (\tau - t_k)}{(\tau - t_k)}$$

$$\left. + \underline{\psi}_{4k} \frac{1}{(\tau - t_k)} \right] d\tau \tag{3.8-64}$$

$$\underline{K}_{21k} (t_k, t_o) = \int_{t_o}^{t_k} \left[D(t_k, \tau) \, \underline{F}_2(\tau) - \underline{\psi}_{1k} \frac{\log Q_k (\tau - t_k)}{(\tau - t_k)^3} \right.$$

$$- \underline{\psi}_{2k} \frac{1}{(\tau - t_k)^3} - \underline{\psi}_{3k} \frac{\log Q_k (\tau - t_k)}{(\tau - t_k)^2}$$

$$- \underline{\psi}_{4k} \frac{1}{(\tau - t_k)^2} - (\underline{\psi}_{5k} + 3 \underline{\psi}_{7k}) \frac{\log Q_k (\tau - t_k)}{(\tau - t_k)}$$

$$\left. - (\underline{\psi}_{6k} + 3 \underline{\psi}_{8k}) \frac{1}{(\tau - t_k)} \right] d\tau \tag{3.8-65}$$

The formulas (3.2-36) through (3.2-52) arise mainly from the expansion of the first-order solution, $\underline{r}_1$, in the overlap domain while those given by (3.2-53) through (3.2-65) arise from a similar expansion of the second-order solution, $\underline{r}_2$. The constants must be evaluated sequentially starting from the relative velocity as given by (3.8-1).

The integral constants $\underline{K}_{10k}$, $\underline{K}_{11k}$, $\underline{K}_{20k}$, and $\underline{K}_{21k}$ must be evaluated numerically using Gaussian quadrature or some similar technique. This requires the integrands to be evaluated at a series of discrete points. The first-order integrands are functions of the two-body solution, $\underline{r}_0$, the partial derivative matrices B and D evaluated along $\underline{r}_0$, and the positions of the N-2 perturbing bodies as given by an ephemeris, as well as the indicated constants. The second-order integrands are similar except that they also depend on the first-order solution, $\underline{r}_1$, which is given by (2.1-13). Since $\underline{r}_1$ itself contains an integral function, the formulas for $\underline{K}_{20k}$ and $\underline{K}_{21k}$ are actually double integrals. This complicates the application of a technique such as Gaussian quadrature since each quadrature point of the outer integral must be divided into n points for the inner integral. An approximation for $\underline{r}_1$ which reduces $\underline{K}_{20k}$ and $\underline{K}_{21k}$ to single integrals is discussed in Volume 2. In addition, Volume 2 contains explicit formulas for the partial derivative matrices A, B, C, and D which must be evaluated to obtain the constants of the outer solution.

The inner constants can be combined to give

$$\underline{\varkappa}_k = M_k \left\{ \underline{L}_k - \left[\tau_k + \frac{Q_k}{\overline{n}_k} \log \frac{M_k \overline{e}_k}{2 \overline{n}_k} \right] \underline{V}_{\infty k} \right\} \tag{3.8-66}$$

while the outer constants can be combined to give

$$\underline{Y}_k = - \underline{\beta}_{1k} (\Gamma_k - 1) - \underline{K}_{10k} (t_k, t_o) \tag{3.8-67}$$

$$\underline{\delta}_k = - \underline{\beta}_{1k} (t_o - t_k)^{-1} - \underline{K}_{11k} (t_k, t_o) \tag{3.8-68}$$

$$\underline{\zeta}_k = \underline{\psi}_{1k} (\Gamma_k + 1)(t_o - t_k)^{-1} + \underline{\psi}_{2k} (t_o - t_k)^{-1}$$

$$+ \underline{\psi}_{4k} (\Gamma_k - 1) - \underline{K}_{20k} (t_k, t_o) \tag{3.8-69}$$

$$\underline{\eta}_k = - \underline{\psi}_{1k} (2\Gamma_k + 1)(t_o - t_k)^{-2}/4 - \underline{\psi}_{2k} (t_o - t_k)/2$$

$$- \underline{\psi}_{4k} (t_o - t_k) + \underline{\psi}_{5k} \left(\Gamma_k^2 - 2\right)/2$$

$$+ \underline{\psi}_{6k} (\Gamma_k + 1) + 3\underline{\psi}_{7k} \left(2\Gamma_k^2 - 5\right)/4$$

$$+ \underline{\psi}_{3k} (3\Gamma_k - 1) - \underline{K}_{21k} (t_k, t_o) - \underline{e}_{1k} + \underline{A}_{k2}^{*}$$

$$- M_k \tau_k \left(\underline{f}_{1k} + 2\underline{g}_{1k} - \underline{p}_k^{*} + \frac{1}{2} M_k \tau_k G_k \underline{V}_k\right) \tag{3.8-70}$$

The only other quantities which appear in the boundary value solutions are the partial derivative matrices obtained by partitioning the state transition matrix, the constants M_k defined by (2.1-7), the dimensionless mass of the $k\underline{th}$ body, μ_k, and the reference mass, μ. As noted previously, many forms for the partial derivative matrices are available. Some are in Cartesian coordinates and can be used directly. Other forms require coordinate transformations to obtain the Cartesian expressions. The expressions which are given in Volume 2 are in Cartesian coordinates.

The two impulse moon-to-Earth solution has not been derived from the fundamental solution and thus requires additional formulas to define the parameters appearing in the solution. The hyperbolic solution between the first and second impulses is defined by the following set of orbital elements and angles:

$$\underline{\ell} = \underline{R}_M (S_1) \times \underline{V}_M (S_1^{+}) \tag{3.8-71}$$

$$\underline{N} = \underline{\ell} / |\underline{\ell}| \tag{3.8-72}$$

$$\bar{h} = \frac{V_M(S_1^+)^2}{2} - \frac{1}{R_M(S_1)} \qquad (3.8\text{-}73)$$

$$\bar{a} = 1/(2\bar{h}) \qquad (3.8\text{-}74)$$

$$\bar{e} = (1 + 2\bar{h}|\underline{\ell}|^2)^{1/2} \qquad (3.8\text{-}75)$$

$$\bar{i} = \cos^{-1}(\underline{N} \cdot \underline{e}_3) \qquad (3.8\text{-}76)$$

$$\sin\bar{\Omega} = \frac{\underline{N} \cdot \underline{e}_1}{\sin\bar{i}} \qquad (3.8\text{-}77)$$

$$\cos\bar{\Omega} = -\frac{\underline{N} \cdot \underline{e}_2}{\sin\bar{i}} \qquad (3.8\text{-}78)$$

$$\sinh\bar{F}_1 = \frac{\underline{R}_M(S_1) \cdot \underline{V}_M(S_1^+)}{\bar{a}^{1/2}\,\bar{e}} \qquad (3.8\text{-}79)$$

$$\cosh\bar{F}_1 = \frac{\bar{a} + R_M(S_1)}{\bar{a}\,\bar{e}} \qquad (3.8\text{-}80)$$

$$\sin\bar{f}_1 = \frac{\bar{a}(\bar{e}^2 - 1)^{1/2}\sinh\bar{F}_1}{R_M(S_1)} \qquad (3.8\text{-}81)$$

$$\cos\bar{f}_1 = \frac{\bar{a}(\bar{e} - \cosh\bar{F}_1}{R_M(S_1)} \qquad (3.8\text{-}82)$$

$$\sin\tilde{\omega} = \frac{[\underline{e}_3 \times \underline{N} \times \underline{R}_M(S_1)] \cdot \underline{N}}{R(S_1)\sin\bar{i}} \qquad (3.8\text{-}83)$$

$$\cos \tilde{\omega} = \frac{\left[\underline{e}_3 \times \underline{N} \cdot \underline{R}_M (S_1) \right]}{R(S_1) \sin \overline{i}} \tag{3.8-84}$$

$$\overline{\omega} = \tilde{\omega}_1 - \overline{f}_1 \tag{3.8-85}$$

$$\overline{n} = (\overline{a})^{-3/2} \tag{3.8-86}$$

$$\overline{U}' = - (|\underline{\ell}| \sin \overline{\omega} + \overline{a}^{1/2} \cos \overline{\omega})/(\overline{a}\overline{e}) \tag{3.8-87}$$

$$\overline{V}' = (|\overline{\ell}| \cos \overline{\omega} - \overline{a}^{1/2} \sin \overline{\omega})/(\overline{a}\,\overline{e}) \tag{3.8-88}$$

$$\overline{U} = \overline{U}' \cos \overline{\Omega} - \overline{V}' \sin \overline{\Omega} \cos \overline{i} \tag{3.8-89}$$

$$\overline{V} = \overline{U}' \sin \overline{\Omega} + \overline{V}' \cos \overline{\Omega} \cos \overline{i} \tag{3.8-90}$$

$$\overline{W} = \overline{V}' \sin \overline{i} \tag{3.8-91}$$

$$\underline{V}_\infty = (\overline{U}, \overline{V}, \overline{W}) \tag{3.8-92}$$

The orbital elements are: $\overline{a}$, the semimajor axis; $\overline{e}$, the eccentricity; $\overline{i}$, the inclination; $\overline{\Omega}$, the argument of the ascending node; $\overline{\omega}$, the argument of pericenter; and the initial inner time is given by (3.5-7). These elements and the initial time are sufficient to define $\underline{R}_{MO}(S)$ and $\underline{V}_{MO}(S)$ in a number of ways, (2.2-11) being one example.

The perturbations to hyperbolic motion, which appear in (3.5-9) and (3.5-10) require the additional formulas

$$G_M = G(\underline{p}_M (t_1)) \tag{3.8-93}$$

$$\underline{H}_M = \underline{H} (\underline{p}_M (t_1)) \tag{3.8-94}$$

$$\underline{A}_3 = 1/24 \ \underline{H}_M \ \underline{V}_\infty^{\ 2} \tag{3.8-95}$$

The outer solution requires the evaluation of four definite integrals given by

$$\underline{\Gamma}_{10}(t_2, t_e) = \int_{t_e}^{t_2} B(t_2, \tau) \, \underline{F}_1(\tau) d\tau \qquad (3.8\text{-}96)$$

$$\underline{\Gamma}_{11}(t_2, t_e) = \int_{t_e}^{t_2} D(t_2, \tau) \underline{F}_1(\tau) d\tau \qquad (3.8\text{-}97)$$

$$\underline{\Gamma}_{20}(t_2, t_e) = \int_{t_e}^{t_2} B(t_2, \tau) \underline{F}_2(\tau) d\tau \qquad (3.8\text{-}98)$$

$$\underline{\Gamma}_{21}(t_2, t_e) = \int_{t_e}^{t_2} D(t_2, \tau) \underline{F}_2(\tau) d\tau \qquad (3.8\text{-}99)$$

These integrals are similar to $\underline{K}_{10k}$, $\underline{K}_{11k}$, $\underline{K}_{20k}$ and $\underline{K}_{21k}$ which are in the fundamental solution. They must be evaluated numerically using a technique like Simpson's rule or Gaussian quadrature. The first-order integrands are functions of the two-body solution $\underline{r}_o$ obtained from the Lambert solution, the partial derivative matrices B and D evaluated along $\underline{r}_o$, and the positions of the moon and sun. The second-order integrands are similar except that they also depend on $\underline{r}_1$ which, according to (2.1-13), contains an integral function itself. Therefore (3.8-98) and (3.8-99) are actually double integrals and require special care in their evaluation.

3.9 COMMENTS

The boundary value solutions presented in the preceding sections satisfy the objective stated in the introduction. They are explicit solutions which, except for the linear versions of the moon-to-Earth solutions, satisfy the boundary conditions exactly without requiring any iterative techniques. Thus they offer a distinct advantage over numerical methods which depend on iterative techniques to converge to the boundary value solution. It should be pointed out however that satisfying the boundary conditions exactly with an approximate solution (which the asymptotic solution does) is not quite the same as satisfying the boundary conditions approximately with an exact solution (as numerical integration does). Since the asymptotic solution is only approximate, an exact solution based on the asymptotic initial conditions will most likely not satisfy the terminal boundary conditions exactly. The difference between the two methods is the subject of the next part of this report.

Section 4
NUMERICAL RESULTS

In order to determine the accuracy of the asymptotic boundary value
solutions, a number of comparisons were made with numerically integrated
trajectories. Prescribed sets of boundary conditions were used to evaluate
the asymptotic solutions for Earth-to-moon, moon-to-Earth, and inter-
planetary applications. Initial conditions determined by the asymptotic solu-
tions were then used in an N-body numerical integration program. Compari-
sons of terminal conditions between the asymptotic and numerically
integrated solutions are used as measures of the accuracy of the asymptotic
solution. That is, for any terminal condition x the comparisons are given
as Δx where

$$\Delta x = x \text{ (asymptotic)} - x \text{ (numerical integration)} \qquad (4\text{-}1)$$

4.1 EARTH-TO-MOON TRAJECTORIES

Earth-to-moon trajectories of the type shown in Figures 2, 3, and 4 and
discussed in Subsections 3.2 and 3.3 were compared with numerical
integration. Initial positions relative to the Earth were determined from
exact solutions of Apollo-type trajectories leaving Earth around February 1,
1971.

Five basic trajectories were considered; with variations in the initial
positions, the total number of trajectories was ten. They cover flight times
from 60 to 100 hours and inclinations at the moon of -35 and -80 degrees
(the minus sign indicating an approach under the moon). The boundary
conditions of all ten examples are given in Table 1.

(Additional trajectories have also been studied but the major conclusions
obtained from the results are similar to those obtained from the trajectories

67

Table 1

BOUNDARY CONDITIONS AND ACCURACIES FOR EARTH-TO-MOON TRAJECTORIES

Trajectory Number	$t_{pM}-t_o$ (hr)	$\underline{r}(t_o)$ (nmi)	$f(t_o)$ (deg)	$\bar{\rho}_M$ (nmi)	$\bar{i}_M$ (deg)	Order	Δt_{pM} (min)	$\Delta\bar{\rho}_M$ (nmi)	$\Delta\bar{i}_M$ (deg)
101	60	3,544	6	1,200	-35	1	11	-18	-0.05
						2	2	-6	0.15
102	80	3,544	10	1,200	-35	1	36	-92	-0.05
						2	-8	-299	-0.33
103	100	3,544	13	1,200	-35	1	45	-210	0.11
						2	-154	-4,497	-2.12
104	59	12,820	118	1,200	-35	1	11	-21	-0.04
						2	3	4	0.08
105	99	12,904	119	1,200	-35	1	*	*	*
						2	-12	-699	-0.65
106	98	21,168	134	1,200	-35	1	47	-162	-0.34
						2	1	-421	-0.45
107	60	3,544	5	1,200	-80	1	11	2	-0.65
						2	-64	-644	-8.86
108	100	3,544	12	1,200	-80	1	46	-94	-4.24
						2	-113	-2,949	-25.90
109	59	12,802	118	1,200	-80	1	11	-11	-0.48
						2	1	-16	0.36
110	98	21,168	134	1,200	-80	1	47	-89	-3.07
						2	3	-353	-7.71

*No Data

presented here. One of the additional trajectories was a 63.5 hour transfer which was very similar to that used by Carlson (Reference 2). The results were in good agreement with his.)

The model for the Earth-to-moon trajectories was a 4-body problem (Earth, Moon, Sun, Spacecraft) with the positions of the moon and sun determined from an analytical ephemeris.

Since the initial positions for five of the ten trajectories lie close to perigee, it was decided to make the comparisons using the nonlinear solution, (3.2-13) through (3.2-19). The linear solution was used first but the results were not satisfactory. The reason for the difference is apparently the fact that the linear solution uses the linear partial derivative matrices. These are not adequate if one of the endpoints lies in the non-linear region of the zeroth-order solution close to perigee. Since the nonlinear solution replaces the transition matrix with an exact zeroth-order Lambert solution, the nonlinear effects are included. As the initial position moves away from perigee the differences between the two solutions are reduced.

The prescribed initial position $\underline{r}(t_o)$ and the calculated initial velocity $\underline{v}(t_o)$ were used as initial conditions in the numerical integration program and the resulting values of pericynthion time, radius, and inclination compared with the prescribed values which are shown on the left side of Table 1. Comparisons were made using both the first- and second-order velocities obtained from (3.2-16) and are shown on the right side of Table 1. The results can be divided into groups which show various trends in the accuracy of the asymptotic solution. The data for each group are presented in the following format.

Group Designation	Case Number	Order of Solution	Δt_{pM}	$\Delta \bar{\rho}_M$	$\Delta \bar{i}_M$

69

The groups are:

A.	101	1	11	-18	-0.05
	102	1	36	-92	-0.05
	103	1	45	-210	-0.11

In this group of three trajectories, the variable boundary condition is the time of flight, and the results show that first-order accuracy is degraded as the time of flight increases.

B.	101	2	2	-6	0.15
	102	2	-8	-299	-0.33
	103	2	-154	-4497	-2.12

In this group, the variable boundary condition is again time of flight but the results are now second order. The same degradation of accuracy as in A is apparent but the degree of degradation is much more marked. For No. 101 the second order is better than the first, but for No. 103, the first order is better.

These results indicate that whatever is degrading the first-order accuracy is having a highly adverse effect on the second-order solution. The cause is most likely the deviation of the first-order solution from the zeroth-order solution. When this deviation is large, as it is in the long-flight-time trajectories, it evidently causes the asymptotic solution to diverge before reaching the second-order term. Thus the second-order error is larger than the first.

C.	101	1	11	-18	-0.05
	104	1	11	-21	-0.04
	101	2	2	-6	0.15
	104	2	3	4	0.08

This group shows the effect of choosing the initial position to be a point one hour out on trajectory No. 101, thus giving No. 104. By delaying the initial position, it occurs at a true anomaly of 118 rather than 6 degrees and at a radius of almost 13,000 rather than 3,544 nautical miles. This delay has little effect on either first- or second-order accuracy.

D.	103	1	45	-210	0.11
	106	1	47	-162	-0.34
	103	2	-154	-4497	-2.12
	105	2	-12	-699	-0.65
	106	2	1	-421	-0.45

This group is similar to C except that the time of flight is near 100 hours rather than 60. A delay of one hour (No. 105) along No. 103 increases the true anomaly by 106 degrees and the radius by 9,360 nautical miles. A delay of two hours (No. 106) increases the true anomaly another 15 degrees and radius another 8,264 nautical miles. The two-hour delay has very little effect on the first order results but the one and two hour delays have a marked effect on the second order results reducing the time of flight error from 154 minutes down to one minute and the radius error from almost 4,500 nmi down to 421 nmi.

Carlson (Reference 2) has shown such a trend in the first-order linear results for a 63.5-hour trajectory (starting at perigee). He shows steps (delays) of 1, 3.5, 8.5, 13.5, 23.5, 33.5, ... hours. Accuracy is improved with each step out to 8.5 hours after which it slowly begins to degrade. He found no such trend using a first-order nonlinear solution, which agrees with the first-order comparisons shown here and in C.

The improvement in accuracy shown here as the initial position is moved away from the Earth is evidently due to a decrease in the deviation between the zeroth- and first-order solutions. This deviation is small for No. 101 thus a delay of one hour has little effect. For No. 103 however, the deviation is initially quite large and delays of one and two hours decrease the deviation and increase the accuracy. The deviation of the solutions can be measured by the magnitude of the first order $\delta \underline{v}(t_o)$. The magnitudes are

No.	Delay (hr)	$\delta v(t_o)$ (ft/sec)
101	0	149
104	1	54
103	0	845
105	1	254
106	2	210

Since neither 101 nor 104 have excessively large values of $\delta v(t_0)$ the second order solutions are not adversely affected. The large value for No. 103, however, results in large second order errors.

E.	107	1	11	2	-0.65
	108	1	46	-94	-4.24

This group is similar to A except the inclination at the moon is -80 rather than -35 degrees and data for the 80-hour trajectory has not been included. The same degradation with increasing time of flight is apparent and, except for inclination, the errors are similar in magnitude to those of A.

F.	107	2	-64	-644	-8.86
	108	2	-113	-2499	-25.90

This group is similar to B except for the difference in inclination and the lack of an 80 hour trajectory. It again shows the degradation of the second-order results as flight time increases but, except for inclination, the degradation is not as marked as in B.

Another trend is also apparent when B and F are considered together as follows:

G.	101	2	2	-6	0.15
	107	2	-64	-644	-8.86
	103	2	-154	-4497	-2.12
	108	2	-113	-2499	-25.90

Comparison of Cases 101 and 107 shows that the second-order accuracy is degraded as the inclination goes from -35 to -80 degrees. Comparison of cases 103 and 108 shows that, except for inclination, the second-order accuracy is improved as the inclination changes. (The anomalous behavior of the inclination cannot be explained.)

Thus inclination at the moon has an effect on the second-order accuracy, the nature of the effect being dependent on the time of flight. No such trend is apparent in the first-order results.

H.	107	1	11	2	-0.65
	109	1	11	-11	-0.48
	107	2	-64	-644	-8.86
	109	2	1	-16	0.36

This group is similar to C except for the difference in inclination. No. 109 is obtained by delaying the starting position one hour along 107. Again the delay has little effect on the first-order results but results in a marked improvement in the second-order results where the errors were originally quite large. The reason for the improvement is discussed in D.

I.	108	1	46	-94	-4.24
	110	1	47	-89	-3.07
	108	2	-113	-2949	-25.90
	110	2	3	-353	-7.71

This group is similar to H except that the time of flight is near 100 hours rather than 60. The trend is identical to H. A delay of two hours has little effect on the first-order results but a significant effect on the second-order results. The reason is again the same: an initial position further from the Earth reduces the deviation between the zeroth- and first-order solutions and thus increases the accuracy.

Several observations can be drawn from A through I and from Table 1 as a whole. The first would be that the second-order solution is much more sensitive to boundary conditions than is the first order. For instance first-order pericynthion radius errors range from -210 to +2 nmi while the second-order errors range from -4,497 to +4 nmi. In some cases the second order is better than the first; in other cases the first order is better. The point of minimum error for the asymptotic solution is evidently less than second order in some cases, and adding the second-order terms causes the solution to diverge. (In general, an asymptotic expansion in powers of μ will most closely approximate the function which it represents after n terms, and then diverges as n is increased. The optimum value of n is a function of μ and other parameters such as boundary conditions. It is difficult to determine a priori.)

The second observation is that second-order errors are increased by starting the trajectory close to perigee, by increasing the time of flight, and by choosing certain values of inclination at the moon. Each of these effects can be related to the size of the first-order velocity correction

$$\delta \underline{v}(t_0) = \left[\underline{v}_o'(t_o) - \underline{v}_o(t_o) \right] / \mu \qquad (4.1-2)$$

When the magnitude $\delta v(t_o)$ is large the error is large and when the magnitude is small the error is small. When $v(t_o)$ is large, the first-order solution $\underline{r}_1$ tends to grow rapidly with time. From (2.1-6) it can be seen that the force $\underline{F}_2''$ is a function of $\underline{r}_1^2$ and this results in large values of the second-order integrals $\underline{K}_{20M}$ and $\underline{K}_{21M}$. Since

$$r_1 = (\underline{r} - \underline{r}_o)/\mu \qquad (4.1.3)$$

its effect could be reduced by choosing $\underline{r}_o$ to be closer to the actual trajectory $\underline{r}$. However, the condition dictated by (2.2-4) prohibits $\underline{r}_o$ from being chosen arbitrarily, i.e., it must pass through the center of the moon. If (2.2-4) is relaxed then it might be possible to choose an $\underline{r}_o$ which would minimize (4.1-3) but such a step causes rather severe complications in the analytical derivation of the solution and is not well enough understood at this point to make any modifications along this line. (For a further discussion of (2.2-4) see Section A10 and the first parts of Sections A11 and A17 in Volume 2.)

The magnitude of $\delta \underline{v}(t_o)$ should be proportional to the perturbations experienced over the entire length of the trajectory. Numerically integrated trajectories show a variation in the orbital elements of less than 10^{-5} over the first two hours of flight after leaving perigee, indicating that the moon and sun perturbations are small over this interval. The large changes in the magnitude of $\delta \underline{v}(t_o)$ as the starting point moves away from perigee (cf., D) must therefore be attributed to something other than the effect of the moon and the sun. The evidence indicates that the cause is the large difference between $\underline{r}_o$ and $\underline{r}_o + \mu \underline{r}_1$, i.e., a fictitious force arises when $\underline{r}_o$ is a poor approximation to the actual solution.

Since a delay in the starting position to one or two hours after perigee never degrades the accuracy but tends to improve it when the errors are large, and since the effect of the real perturbing forces is small over the initial one- or two-hour interval it may be possible to construct a more uniformly valid solution by applying either a two-body or a perturbed two-body solution out to a true anomaly of 120 to 135 degrees and then applying the asymptotic boundary value solution from there to the moon. Certain modifications would be required to make the velocity continuous between the two solutions, but such changes are relatively minor. Lack of time prohibited making such a modification in this study although a somewhat related solution was incorporated into the interplanetary solution. It is termed the modified linear solution in Subsection 3.7 and the results are shown in Subsection 4.4.

A third observation is that since accuracy is increased as the starting point is moved away from perigee, the midcourse application is probably better than the full Earth-to-moon application. This is especially true if a simple form of the asymptotic solution is desired, since it has been amply pointed out that starting from perigee probably will require a composite solution to obtain uniform accuracy.

The fourth and final observation is that starting at perigee will always involve rather large sensitivities to initial errors. The initial velocity calculated, even without any modification, may differ by only a small amount from the actual velocity which satisfies the boundary value problem exactly. Whether or not these small differences are tolerable depends on the particular use to which the solution is being applied.

4.2 TWO-IMPULSE MOON-TO-EARTH TRAJECTORIES

Two-impulse moon-to-Earth trajectories of the type shown in Figures 7 and 8 and discussed in Subsection 3.5 were also compared with numerical integration. The initial position and velocity were taken from a patched conic optimum 4-impulse solution obtained from NASA-MSC. The initial time was zero hours on February 8, 1980 (Julian Date 2444277.5) and the initial position and velocity were

$$\underline{R}_{M1} = (263.24, -923.75, 272.72) \text{ nautical miles} \qquad (4.2\text{-}1)$$

$$\underline{V}_{M1}^{-} = (-1125.44, 1181.10, 5086.90) \text{ feet/second} \qquad (4.2\text{-}2)$$

This corresponds to a 60-nmi circular orbit about the moon with an inclination of 97.582 degrees. The first impulse was chosen to match the patched conic solution by putting

$$I_1 = 0.45805 \qquad (4.2-3)$$

This resulted in a hyperbolic orbit after the first impulse with a pericenter radius of 998.49 nmi, an eccentricity of 1.1259, and the same inclination as before.

Equations (3.5-8) and (3.5-9) were used to determine the position and velocity at five-hour intervals out to 25 hours. The magnitudes of the two-body position and velocity, R_{Mo} and V_{Mo}, the position and velocity perturbation, δR_M and δV_M, and the errors when compared to numerical integration, $|\delta \underline{R}_M|$ and $|\delta \underline{V}_M|$, are shown in Table 2. The results show the solution defined by (3.5-8) and (3.5-9) to be quite accurate with position and velocity errors running 0.1 percent or less. It is interesting to note that at 20 hours the predicted radius was approximately the radius of the moon's sphere of influence and the perturbations δR_M and δV_M indicate the error of a patched conic solution at this point.

Table 2
POSITION AND VELOCITY MAGNITUDES AND
ERRORS OF PERTURBED HYPERBOLA

$t_2 - t_1$ (hr)	R_{M0} (nmi)	$\delta \underline{R}_M$ (nmi)	$|\underline{\Delta R}_M|$ (nmi)	V_{M0} (fps)	δV_M (fps)	$|\underline{\Delta V}_M|$ (fps)
5	10,842	5.7	0.9	2,975	4.9	0.4
10	18,797	39.6	5.1	2,574	17.4	0.8
15	26,070	124.0	13.2	2,404	37.2	1.1
20	32,992	281.4	24.9	2,307	64.6	1.0
25	39,694	535.2	39.7	2,243	100.0	2.5

At each of the five points in Table 2, a second impulse was calculated using the linear solution (3.5-19). Entry times were chosen to make the total flight time, $t_e - t_1$, equal to 120, 100, and 80 hours. In addition, an impulse was added at $t_2 - t_1 = 5$ hours which resulted in a 60-hour flight time. (Flights of 60 hours flight time from $t_2 - t_1 = 10$, 15, 20, and 25 hours were not possible without going to hyperbolic transfers. This was because $t_e - t_2$ for each of these points was less than the parabolic flight time from that point to Earth.) These trajectories are summarized in Table 3. They are grouped according to the time of the second impulse in order of decreasing total flight time. Magnitudes of the second velocity impulse are shown, the magnitude of the first impulse was the same for all cases, i.e.,

$$\Delta V(t_1) = 2,447 \text{ fps} \qquad (4.2-4)$$

The Earth entry conditions were

$$r_e = 3,594 \text{ nmi} \qquad (4.2-5)$$

$$\gamma_e = 0.0 \text{ deg} \qquad (4.2-6)$$

$$i_e = 30.0 \text{ deg} \qquad (4.2-7)$$

The choice of zero for γ_e meant that entry coincided with perigee. Errors in perigee time, radius, and inclination are shown as well as errors in entry time and flight path angle for those trajectories where the numerically integrated solution passed through the entry radius, i.e., had positive perigee radius errors meaning the numerically integrated perigee was below the perigee (entry) radius.

The numerical integration program was set to cut off at flight times of 125 hours. In the cases where this limit was reached, the radius at that time is shown to give an indication of how far off the trajectory was.

Table 3

TIME INTERVALS, VELOCITY IMPULSES, AND ACCURACIES FOR TWO-IMPULSE MOON-TO-EARTH TRAJECTORIES (Page 1 of 2)

Trajectory Number	$t_e - t_1$ (hr)	$t_2 - t_2$ (hr)	Order	$\Delta V(t_2)$ (fps)	Δt_p (min)	Δr_p (nmi)	Δi_p (deg)	Δt_e (min)	$\Delta \gamma_e$ (deg)
201	120	5	0	960		$r(125) = 54,011$ nmi			
			1	2,014		$r(125) = 19,263$ nmi			
			2	2,838		$r(125) = 94,324$ nmi			
202	100	5	2	1,450	4	-1,266	-22.0	*	*
203	80	5	2	1,861	42	463	-13.5	45	-21
204	60	5	2	3,647	17	410	-6.5	20	-20
205	120	10	0	1,013		$r(125) = 9,835$ nmi			
			1	1,648	-88	-1,971	-6.2	*	*
			2	1,828	-180	-4,155	-9.5	*	*
206	100	10	2	1,225	16	160	-6.0	18	-12
207	80	10	2	1,937	12	243	-3.0	14	-15
208	120	15	0	1,092	-169	-3,424	15.7	*	*
			1	1,515	-29	-640	-2.9	*	*
			2	1,583	-41	-978	-5.0	*	*
209	100	15	2	1,186	8	139	-2.4	10	-11
210	80	15	2	2,102	4	123	-1.2	6	-11

*Numerically integrated perigee radius is greater than prescribed entry radius and no entry occurs.

Table 3

TIME INTERVALS, VELOCITY IMPULSES, AND ACCURACIES FOR
TWO-IMPULSE MOON-TO-EARTH TRAJECTORIES (Page 2 of 2)

Trajectory Number	t_e-t_1 (hr)	t_2-t_1 (hr)	Order	$\Delta V(t_2)$ (fps)	Δt_p (min)	Δr_p (nmi)	Δi_p (deg)	Δt_e (min)	$\Delta \gamma_e$ (deg)
211	120	20	0	1,162	-108	-2,266	12.0	*	*
			1	1,462	-11	-246	-1.4	*	*
			2	1,494	-12	-295	-2.6	*	*
212	100	20	0	950	-84	-1,750	10.1	*	*
			1	1,176	2	32	-0.5	3	-5
			2	1,189	5	97	-1.2	6	9
213	80	20	0	2,227	-48	-1,153	7.4	*	*
			1	2,310	1	23	-0.2	2	-5
			2	2,314	2	75	-0.6	4	-8
214	120	25	0	1,225	-72	-1,623	9.3	*	*
			1	1,447	-2	-99	-0.8	*	*
			2	1,465	-1	-87	-1.5	*	*
215	100	25	2	1,212	5	73	-0.7	6	-8
216	80	25	2	2,577	2	56	-0.5	3	-7
217	120	6.3	**	539	-189	-4,877	4.7	*	*

*Numerically integrated perigee radius is greater than prescribed entry radius and no entry occurs.

**Patched conic solution obtained from NASA-MSC.

The results shown are second-order results except for the 120-hour flights and the flights where the second impulse occurred at the sphere of influence. In these cases zeroth, first- and second-order results are all shown. (The order of the solution applies only to the phase after the second impulse. The hyperbolic phase used the perturbed solution in all cases since the accuracy of this phase had already been determined.)

The results show three basic trends. First, as $t_2 - t_1$ increases with $t_e - t_1$ held fixed, the accuracy improves. This is to be expected. As the point of the second impulse moves away from the moon, the outer solution which is used to derive (3.5-19) becomes a better approximation to the actual solution. If the initial point is too close to the moon (a distance of order μ) then the outer solution must be replaced by a matched solution obtained from the fundamental solution. Since the primary purpose of the two-impulse solution is to study trajectories where the second impulse occurs away from the moon, the derivation was made accordingly. Thus values of $t_2 - t_1$ of 5 and even 10 hours represent marginal applications for this type of solution, and the errors are not entirely unexpected.

The second trend occurs when $t_2 - t_1$ is held fixed and $t_e - t_1$ decreased. The trend in each group is toward improved accuracy. This should also be expected if the Earth-to-moon results of the previous section are considered. It was shown there that increasing flight time degraded accuracy. The same trend appears here with decreasing flight time giving increased accuracy.

The cause is probably the same as in the Earth-to-moon cases, i. e. , the deviation of the first-order solution from the zeroth-order solution increases with increasing flight time and adversely affects the accuracy. A second cause may be the use of the linear rather than the nonlinear solution. All of the post-second impulse trajectories had transfer angles between 170 and 180 degrees, the 120-hour trajectories all being around 178 degrees. The linear partial derivative matrices may introduce considerable error in such cases since both end points lie in highly nonlinear regions of the zeroth-order solution. Since the nonlinear solution does not use the partial derivative

matrices (except in the definite integrals), it could be expected to give better results. Time did not permit an evaluation of the nonlinear solution.

The third trend apparent is that the first-order solution gives better results than the second order in all but one of those cases where the zeroth-, first-, and second-order solutions have all been compared with numerical integration. However, a comparison of Cases 201, 205, 208, 211, and 214 shows that the difference between the first- and second-order solutions is decreasing as $t_2 - t_1$ increases and finally when $t_2 - t_1$ equals 25 hours the second order is better. This also can be attributed to the size of the deviation between the zeroth- and first-order solutions. When this deviation is large, as it is when the second impulse occurs close to the moon, then the second-order accuracy is adversely affected. As the deviation decreases, the adverse effect is diminished and the second-order accuracy is improved.

The cases where $t_2 - t_1$ equals 20 hours, Cases 211 to 213, are interesting since the zeroth-order results are nearly equal to what a patched conic solution would give. Prior to the second impulse, the solution is a perturbed hyperbola, but the perturbations are not excessively large and the solution is close to a pure two-body solution. After the second impulse, the zeroth-order solution is a two-body ellipse. Since the second impulse occurs at the sphere of influence, the zeroth-order solution is nearly patched conic (actually slightly more accurate). The results show that both the first- and second-order solutions are an order of magnitude more accurate than the zeroth-order solution and that the zeroth-order solution predicts a velocity impulse which is less than that actually required to satisfy the boundary conditions. This would indicate that patched conic solutions may give considerable error if used to determine the optimum time for adding the second impulse.

This point is emphasized by considering No. 217. The errors for this case were obtained by numerically integrating from the initial conditions predicted by the patched conic program used at NASA-MSC and adding the indicated impulse at 6.3 hours. Although the solution is supposedly optimum, the

terminal errors are quite large and the second impulse would probably have to be increased by several hundred feet per second to cancel out the errors. The magnitude of the second impulse would then approach that of No. 209 which was the minimum of all the second-order impulses calculated by the asymptotic solution. However, for No. 209 the second impulse occurs 8.7 hours later and the total flight time is 20 hours less than No. 217, indicating quite a change in the possible optimum conditions.

A final observation is that the errors in time of flight, perigee radius and entry flight path angle shown in Table 3 are never as small as one might expect from a second-order theory. As discussed previously, the overall accuracy could be expected to improve by going to a nonlinear solution, but problems pertaining to sensitivity might still remain. Thus, as in the Earth-to-moon solution, the intended use of the solution will determine to a large extent what accuracies are acceptable. If the accuracies shown here, particularly those for long flight times, are unacceptable then further numerical analysis would be warranted to see if the errors could be reduced by either using the nonlinear solution or by formulating a composite solution in which the deviations from the zeroth-order solution are less. This latter approach would be similar to the combined two-body/asymptotic solution suggested for Earth-to-moon trajectories.

4.3 INTERPLANETARY MIDCOURSE TRAJECTORIES

Interplanetary trajectories of the type shown in Figure 9 and discussed in Subsection 3.6 were compared with numerical integration. Two Earth-to-Mars reference trajectories were chosen; the first was a 244-day transfer leaving Earth on November 11, 1964 and the second a 184-day transfer leaving Earth on May 19, 1971. The first reference trajectory was used by Carlson (Reference 2) and is presented here for comparison with his results. The second reference trajectory is similar to that actually flown by the 1971 Mariner mission.

The prescribed boundary conditions at Mars are shown in Table 4. The initial positions were determined along two-body solutions intersecting Earth and Mars at the departure and arrival dates. The initial velocity was

Table 4

TERMINAL BOUNDARY CONDITIONS FOR MIDCOURSE-TO-MARS TRAJECTORIES

Reference Trajectory	t_{PT} (Date)	(Hour)	$\bar{\rho}_T$ (nmi)	$\bar{i}_T$ (deg)
1964–244 Day	July 13, 1965	11:59:45	1,898	33.9
1971–184 Day	Nov 19, 1971	12:00	2,000	30.0

then calculated using the linear solution. The position and velocity were used as initial conditions in the numerical integration program and the resulting boundary conditions compared with the predicted values. The comparisons are shown in Table 5, Cases 301 to 306 corresponding to initial positions along the 1964 244-day trajectory, and Cases 307 and 308 corresponding to initial positions along the 1971 184-day trajectory. The time to go to pericenter and the distance from Mars are shown for each initial position as well as the differences (errors) in pericenter time, radius, and inclination.

The model used was a seven-body problem with the positions of Venus, Earth, Mars, Jupiter, and Saturn obtained from an analytical ephemeris.

The 1964 reference trajectory is a relatively low-energy Earth-to-Mars transfer with a heliocentric transfer angle of about 178 degrees. The six midcourse points, 40 days apart, correspond to some of the initial positions investigated by Carlson (Reference 2). In each case both first- and second-order results are shown.

The first-order comparisons agree very well with Carlson's first-order results. They show an increasing degree of accuracy from 220 to 100 days and then a trend toward decreasing accuracy as the time of flight is further reduced below 100 days. The large error at 220 days can be attributed to

Table 5

ACCURACIES FOR MIDCOURSE-TO-MARS TRAJECTORIES

Trajectory Number	$t_{pT}-t_o$ (days)	$\|\underline{r}(t_o)-P_T(t_T)\|$ (nmi)	Order	Δt_{pT} (sec)	$\Delta \bar{\rho}_T$ (nmi)	$\Delta \bar{i}_T$ (deg)
301	220	104.4×10^6	1	-218.0	192.5	-0.470
			2	52.9	50.1	-0.012
302	180	70.9×10^6	1	-8.3	0.3	0.000
			2	-0.9	-1.0	0.001
303	140	44.1×10^6	1	-4.7	-0.9	0.000
			2	-0.2	-0.5	0.001
304	100	25.4×10^6	1	-4.9	0.0	-0.001
			2	-0.2	-0.5	0.002
305	60	13.0×10^6	1	-6.2	0.7	-0.001
			2	-0.1	-0.3	0.001
306	20	4.1×10^6	1	-13.5	2.4	0.000
			2	-0.2	0.1	0.000
307	123	25.4×10^6	0	-3,909.6	-2,061.7	-5.284
			1	54.0	3.9	-0.001
			2	28.8	11.6	-0.001
308	61	8.8×10^6	0	9,817.2	1,986.5	-186.982
			1	39.6	-5.3	-0.000
			2	3.6	-1.3	-0.000

several causes but the most probable is that the starting point is in a region relatively close to the Earth where the midcourse solution may not be applicable. That is, the assumptions used to derive the midcourse solution are not satisfied if one of the perturbing bodies other than the target body is relatively close to the starting point. If the starting point is within a distance of order μ of such a perturbing body then the interplanetary solution of Section 3.7 must be used. The starting points for Cases 301 and 302 evidently lie between the domain of validity of the two solutions. The increasing error as $t_{pT}-t_o$ goes below 100 days can be attributed to certain terms proportional to $(t_{pT}-t_o)^{-1}$ which are ignored in the first-order solution.

The second-order solution shows a definite improvement in accuracy for Cases 301 and 306. In Cases 302 to 305 the second-order shows an improvement in time of pericenter passage but the results for radius and inclination are inconsistent, sometimes better and sometimes worse than the first order. The mixed results for radius and inclination are probably due to the fact that both the first- and second-order values may be within the accuracy limits of the numerical integration itself.

The 1971 reference trajectory is a somewhat higher-energy Earth-to-Mars transfer with a heliocentric transfer angle of about 142 degrees. The two midcourse points occur two and four months after launch and lie in the region where the midcourse solution can be expected to work well. For each case zeroth-, first-, and second-order results are shown.

The zeroth order solution, which is identical to the massless planet conic approximation often used for interplanetary trajectory analysis, results in rather large errors. These errors are reduced significantly by the first and second order solutions and, except for the pericenter radius error in Case 307, the second order is better than the first.

The magnitude of the first- and second-order errors in Cases 307 and 308 is difficult to explain. Since the 1971 trajectory is a higher energy one (i.e., has less flight time) than the 1964 trajectory, the results from the lunar trajectories would indicate that the errors should be less. Also the two points are at

distances from Mars which are comparable to Cases 304 to 306. Yet both the first- and second-order errors in Cases 307 and 308 are considerably larger than those in Cases 304 to 306. These differences are evidently due to the combination of time of flight, pericenter radius, and inclination prescribed for each of the reference trajectories, but a detailed inspection of each of the cases does not give any hint as to why this should be so.

The final observation regarding Cases 307 and 308 is that the first- and second-order results show improvement as the time to go decreases. This is in agreement with Cases 301 to 306.

The interplanetary midcourse solution appears to be an excellent application for the asymptotic solution. There are two basic reasons for this. The first is the magnitude of the small parameter μ. In the lunar cases μ is 10^{-2} while in the midcourse-to-Mars application μ is 10^{-7}. This causes the asymptotic expansions to converge much more rapidly.

The second reason is less apparent from a theoretical point of view but just as important as the size of μ: it is the fact that the location of the initial position does not have as strong an effect on accuracy as in the previous results. In the lunar examples the zeroth-order solution has an eccentricity close to unity and the region close to perigee (and apogee) has a highly nonlinear behavior. In interplanetary applications the corresponding eccentricities are 0.25 or less and the initial position, even if close to perihelion, does not lie in a highly nonlinear region.

The combination of small μ and nearly circular zeroth-order outer solutions causes the deviation between zeroth- and first-order solutions to be relatively small when both start from a common position as in the midcourse solution. The results of the next section show that this is no longer true when the initial position is close to another body.

86

4.4 INTERPLANETARY TRAJECTORIES

Interplanetary trajectories of the type shown in Figure 10 and discussed in Subsection 3.7 were also compared with numerical integration. The two reference trajectories are the 1964 and 1971 examples of the previous section except here they are considered in reverse order. The same seven-body model was used.

The prescribed boundary conditions are shown in Table 6. The conditions at Earth are typical of departure from a low-Earth orbit. In Cases 401 and 402 the terminal conditions are typical of a close approach, while in Cases 403 and 404 the pericenter radius at Mars is rather large. This value was chosen since a numerically integrated solution with identical boundary conditions was available for comparison.

For each case, the initial position and velocity at the Earth were calculated from (3.7-14) and (3.7-15) using either the linear or modified linear solution. The position and velocity were then numerically integrated up to a close approach at Mars and the resulting boundary conditions compared with the prescribed values. The comparisons are shown in Table 7.

Case 401 shows zeroth-, first-, and second-order results of applying the linear solution to the 1971 trajectory. The results show the expected improvement going from zeroth to first order but then a significant degradation in accuracy going from first to second order.

Case 402 shows the results of applying the modified linear solution. The midpoint was offset by almost 75,000 nautical miles or 10^{-3} in dimensionless units. The results show that except for zeroth-order inclination and second-order time of pericenter passage, the modified solution caused a slight degradation in accuracy.

Since the zeroth- and second-order solutions showed such large errors for the 1971 trajectory, only the first-order solution was compared with numerical integration for the 1964 trajectory. The first-order results of

Table 6

INITIAL AND TERMINAL CONDITIONS FOR EARTH-TO-MARS TRAJECTORIES

Trajectory Number	t_{pL} (date)	$\bar{\rho}_L$ (nmi)	$\bar{i}_L$ (deg)	t_{pT} (date)	$\bar{\rho}_T$ (nmi)	$\bar{i}_T$ (deg)	Version
401	May 19, 1971	4,000	60	Nov 19, 1971	2,000	30	Linear
402	May 19, 1971	4,000	60	Nov 19, 1971	2,000	30	Modified Linear
403	Nov 11, 1964	3,550	40	July 13, 1965	27,219	23.8	Linear
404	Nov 11, 1964	3,550	40	July 13, 1965	27,219	23.8	Modified Linear

88

Table 7

ACCURACIES FOR EARTH-TO-MARS TRAJECTORIES

Trajectory Number	Heliocentric Transfer Angle (deg)	Midpoint Shift (nmi)	Order	Δt_{p_T} (hr)	$\Delta \bar{\rho}_T$ (nmi)	$\Delta \bar{i}_T$ (deg)
401	142.4	———	0	101.4	-71,702	65.4
			1	8.0	-8,289	-0.5
			2	472.5	-32,370	-9.9
402	142.4	74,642	0	117.5	-83,357	13.5
			1	9.0	-8,819	-0.8
			2	456.7	-32,626	-9.9
403	177.6	———	1	8.7	-22,545	0.8
404	177.6	920,987	1	3.6	-9,005	-2.4

both the linear and modified solutions are given by Cases 403 and 404. The modified solution resulted in a reduction of over 50 percent in the time and radius errors but caused a slight increase in the already small inclination error. The reason that the modified solution gave better results in this example is probably due to the size of the midpoint shift which is 10^{-2} in dimensionless units. Since the midpoint shift was an order of magnitude larger than in the previous example it could be concluded that the linear solution (403) contained significantly more error (than 401) due to the larger deviation from the zeroth-order solution.

It should be pointed out that a solution of any given order has a minimum error associated with that order. Solutions like the modified linear or the nonlinear are only attempts to reduce the error to its minimum value. If the linear solution itself is close to the minimum error then the other solutions will not result in any improvement. This is evidently what happened in Case 402.

The second-order errors are much larger than anticipated and are not removed by going to the modified solution. It is felt that the cause of the large error is twofold. First, as shown in Figure 10, the zeroth-order solutions do not go through the true midpoint in either the linear or modified linear solutions. Therefore there is always a finite difference between zeroth and first order and it has been shown in previous sections that this can cause rather large second-order errors if the deviation becomes large.

In the lunar and interplanetary midcourse solutions, the first-order perturbation, r_1, always vanishes at $t = t_0$ and this helps to reduce the maximum value which r_1 may attain at some later time. In the interplanetary solution such is not the case and the large values which r_1 may attain cause excessively large deviations from zeroth order. In order to illustrate this point consider the difference between the zeroth- and first-order midpoints for Cases 401 and 403. These differences are equal to the midpoint shifts in Cases 402 and 404, i.e., 10^{-3} and 10^{-2}. But according to (3.7-17) the shift in the midpoint should be order μ or 10^{-7}. (If the earth is the reference body then μ would be 10^{-6}. In either case the midpoint shift should be the same, theoretically between 10^{-6} and 10^{-7}.) Even if these differences are reduced by one or two orders of magnitude they still remain larger than order μ and therefore introduce error.

The second cause probably lies in the evaluation of the integral $\underline{K}_{21L}$ which eventually ends up in η_L. In all other solutions which use this integral it is not used in calculating the initial position or velocity. That is, the value of the initial velocity perturbation $\underline{\delta v}(t_0)$ is a function of the first order value of $\underline{V}_{\infty k}$ and the constant $\underline{\eta}_k$ is used only in obtaining the second order value of $\underline{V}_{\infty k}$. This means that $\underline{\eta}_k$ is used only in calculating non-prescribed boundary conditions at the terminal end of the trajectory. In the interplanetary solution, however, $\underline{\eta}_L$ is used to determine the second order value of $\underline{V}_{\infty L}$ [cf. (3.7-10) and (3.7-12)] which in turn is used to determine second order orbital elements and second order position and velocity at the launch planet (cf. (3.7-14), (3.7-15) and Section 3.8). Therefore the importance of the integral $\underline{K}_{21k}$ increases significantly in the interplanetary solution.

Of all the definite integrals which must be evaluated $\underline{K}_{21k}$ is the most difficult because it has the most complex integrand. Since the integrals cannot be evaluated exactly but only by some numerical approximation they always include some error. If they are large then the error is correspondingly large. In Case 402 the magnitude of K_{21L} was 10^8. A one percent error in the Gaussian quadrature would be 10^6. The effect of this error can be determined by multiplying by μ^2 since $\underline{K}_{21L}$ is a second-order integral. The net effect is 10^{-8} or almost order μ! If attempts are made to reduce the error by enough orders of magnitude so that it is no longer a problem, then the computation time increases considerably.

The large second-order errors indicate that a better zeroth-order solution is needed for this application. The first-order solution however, works well and offers considerable improvement over the massless-planet (zeroth-order) approximation. Even though the first-order errors in Cases 401 to 404 may appear somewhat large, the actual initial positions and velocities are quite close to those needed to satisfy the boundary conditions with an exact solution. The errors between the asymptotic solution and numerical integration when both satisfy the boundary conditions are shown for Cases 403 and 404 in Table 8. Notice that in the linear solution (403) the first-order errors are large and the second order actually slightly better. By going to the modified solution (404) the zeroth- and first-order errors are reduced significantly while the second-order errors are reduced only slightly.

The first-order error for Case 404 dramatically illustrates the problem of sensitivity which has been mentioned earlier. Errors of 14 nmi in position and 77 fps in velocity (out of a total velocity of 37, 858 fps) result in errors of 3.6 hours and 9, 005 nautical miles at closest approach to Mars. Since problems of sensitivity cannot be eliminated, the errors shown for first order in Table 8 are probably acceptable.

4.5 COMPUTATION TIMES

The asymptotic solutions require three basic types of calculations: (1) Lambert solutions, (2) Gaussian quadrature, and (3) general calculations including the boundary value solution equations, partial derivative matrices,

Table 8

INITIAL POSITION AND VELOCITY ERRORS
FOR EARTH-TO-MARS TRAJECTORIES

Trajectory Number	Order	$|\Delta R_{pL}|$ (nmi)	$|\Delta V_{pL}|$ (fps)
403	0	601	2,706
	1	84	460
	2	47	321
404	0	96	561
	1	14	77
	2	35	326

conversions to dimensionless numbers, etc. The first two require numerical techniques (including iterations in the Lambert solutions); the third involves straightforward evaluation of explicit expressions. The calculations can be accomplished quite rapidly on a high-speed computer.

FORTRAN programs which evaluate the asymptotic solutions were run on a CDC 6500 computer as was the numerical integration program. In the asymptotic solutions the Lambert problems required approximately 0.3 seconds per solution while a 60-point Gaussian quadrature routine required approximately 0.4 seconds for each of the N-2 perturbing bodies. The total computation times for each of the different solutions as well as the corresponding numerical integration times are shown in Table 9.

In the Earth-to-moon solution a large part of the time is spent in Lambert solutions, while in the interplanetary solutions a considerable portion of the time is spent calculating the effect of the perturbations through the Gaussian quadrature routine. Since the interplanetary solution is derived from two fundamental solutions rather than one, it requires almost twice as much time as the midcourse solution. The modified linear solution adds two additional Lambert solutions plus an extra first-order solution which pushes the time over 10 seconds.

Table 9

COMPUTATION TIMES ON CDC 6500 COMPUTER

Type of Solution	Version	Perturbing Bodies (N-2)	Lambert Solutions	Time (sec)	Numerical Integration Time (sec)	
					Initial Value	w/Hunting Procedure
Earth-to-Moon	Nonlinear	2	5*	3.7	25 to 30	
Two-Impulse Moon-to-Earth	Linear	2	1	1.7	40 to 45	
Interplanetary Midcourse	Linear	5	1	3.4	20 to 25	130 to 150
Interplanetary	Linear	5	1	6.0	80 to 90	
Interplanetary	Mod. Linear	5	3	10.5	80 to 90	

*Includes two iterations on second-order solution

93

Whereas the asymptotic solutions are boundary value solutions, the numerical integration runs with which they were compared are only initial value solutions based on the asymptotic initial conditions. Even so, the computation times for the asymptotic solutions are from 6 to 38 times faster than those for numerical integration. In order to obtain a boundary value solution from numerical integration, a hunting or search procedure must be added which significantly increases the computation time. If the asymptotic solution is then compared with the numerically integrated boundary value solutions, the computation times are 25 to 150 times faster. An actual comparison is shown in Table 9 for interplanetary midcourse trajectories.

It should be noted that computation time is significantly affected by the number of quadrature points needed to evaluate the constants. A 120-day interplanetary midcourse solution was evaluated with 12, 36, 60, and 96 quadrature points. Although computation time varied by almost a factor of three, there was little effect on the accuracy, indicating that, for this trajectory at least, 12 points were sufficient. Thus the computation times shown in Table 9 might be reduced with no significant loss of accuracy by reducing the number of quadrature points.

Finally, the programs used to evaluate the asymptotic solutions are still in the development stage and no real attempt has been made to optimize the computation time. The programs make many calculations which do not affect the solution but which were useful during checkout. It is estimated that by eliminating these unnecessary calculations and making other changes within the program, the computation times could be reduced from 25 to 50 percent.

4.6 DISCUSSION OF NUMERICAL RESULTS

The numerical results presented here consist of a limited number of examples from which various trends in accuracy can be observed. These trends are felt to be representative of the accuracies which result from the different boundary value solutions, but it may be that a more comprehensive numerical analysis might reveal further information.

The examples for which data is presented include those which were used as
test cases in checkout of the computer programs for each solution. This
process went through the following sequence of solutions:

1. Linear first-order midcourse interplanetary
2. Linear first-order interplanetary
3. Linear second-order midcourse interplanetary
4. Linear second-order interplanetary
5. Modified linear second-order interplanetary
6. Linear second-order Earth-to-moon
7. Nonlinear second-order Earth-to-moon
8. Linear second-order two-impulse moon-to-Earth.

Since the analytical derivations of each solution preceded the coding and
checkout by several months, the derivation of the final solution (8) was
completed while the coding and checkout of 4 was taking place. Also, by the
time results were being obtained from 6 and 7, the coding of 8 had been
completed. Since many of the factors influencing the asymptotic solution
were determined from the numerical analysis of 6 and 7 and since this
analysis occurred late in the study period, there was not sufficient time to
develop a more comprehensive numerical survey and make changes in the
other solutions.

The sequence of solutions did reveal two aspects of the asymptotic solution
which need to be re-emphasized. The first is the need for a better nominal
or zeroth-order outer solution in order to decrease the deviation between
it and the first order solution. An attempt was made to improve the nominal
in the linear midcourse interplanetary solution. The new nominal did not go
through the center of the target body and thus (2.2-4) was violated. This
caused singularities in the definite integrals and therefore an invalid solution.
This was corrected by introducing a fictitious body with the mass of the
target body but with a slightly different position in order to make the new
nominal satisfy (2.2-4). This new solution did give slightly better
results for Cases 301 and 302 and eventually led to the inclusion of the
nonlinear versions of each solution. [The nonlinear versions were first
discussed by Carlson (Reference 2) but were not emphasized strongly.]

The second characteristic which was revealed was that the form of the fundamental solution can affect the accuracy. It was mentioned in Subsection 2.6 that the form chosen was not unique and was slightly different than the results of Carlson (Reference 2). A more comprehensive numerical survey should include different versions based on these differences in the fundamental solution.

A general comment regarding all of the solutions is that attempts to improve accuracy, by whatever means, sometimes results in an improvement in one boundary condition and a degradation in another. This makes it somewhat difficult to assess the value of the supposed improvement without studying a large number of cases.

It would appear from the results obtained in the preceding sections and from the comments of this section that a more comprehensive numerical survey of all of the solutions is needed. Such a survey should be based essentially on the solutions as they have been derived but including all versions of each solution and those changes, such as the construction of a composite-type solution, which have been specifically mentioned previously.

Section 5

CONCLUSIONS AND RECOMMENDATIONS

5.1 CONCLUSIONS

The analytical solutions presented in this report are a result of combining and extending the best ideas put forth in previous works on this subject. The solution of Reference 1 stressed the mathematical rigor and explicitness of results which evolved from the earlier work of Lagerstrom and Kevorkian. Reference 2, while also stressing a certain degree of explicitness, was based on a more general solution first derived by Breakwell and Perko. The concepts of mathematical rigor, explicitness, and generality have been combined in this study to generate a number of asymptotic solutions for both lunar and interplanetary applications. The basic solutions are the second order outer and inner solutions presented in Subsections 2.1 and 2.2. These solutions are themselves useful for studying motion along perturbed ellipses and hyperbolas, respectively; however, their main purpose in this study lies in the formulation of general solutions for trajectories which have both elliptic and hyperbolic behavior, with a continuous transition from one to the other.

The fundamental solution presented in Subsection 2.5 represents the result of matching the second-order outer and inner solutions in the overlap domain (i.e., the region of transition from elliptic to hyperbolic motion). This solution is valid for any number of perturbing bodies and represents the first matched asymptotic solution which has been carried to second order.

Several boundary value solutions have been formulated directly from the fundamental solution. These include the Earth-to-moon solutions (Subsections 3.2 and 3.3) and the interplanetary midcourse solution (Subsection 3.6). These solutions are second-order approximations to the exact

solution and satisfy the prescribed boundary conditions (both initial and terminal) exactly without need for any iterative techniques (other than in the Lambert solutions).

Two fundamental solutions have been combined to formulate the interplanetary solution of Subsection 3.7. Like the other boundary value solutions it is N-body, second-order, and non-iterative. It is valid for all trajectories originating close to one planet and terminating close to another.

A modified version of the fundamental solution has been used to formulate the one-impulse moon-to-Earth solution (Subsection 3.4). In addition, separate versions of the second-order inner and outer solutions have been used directly (no fundamental solution) to formulate the two-impulse moon-to-Earth solution (Subsection 3.5).

Although applicable to a number of boundary value problems, all of the solutions presented are similar in that they are represented analytically in the form of asymptotic expansions. Also, the solutions have been derived so that most of the mathematical operations required for numerical evaluation are common to each formulation and all of the solutions can be programmed as subroutines of a master trajectory program.

The primary purpose of this study was the development of analytical boundary value solutions. Nevertheless, Section 4 contains sufficient comparisons with numerical integration to demonstrate the accuracy and speed of the asymptotic solution in typical applications. For each solution evaluated, the results showed a significant improvement in accuracy over standard conic approximations. In one application (i. e., interplanetary midcourse the accuracy is comparable to that of numerical integration. (In fact, the results of the asymptotic solution pointed out a deficiency in the numerical integration program with which it was being compared. Introduction of more stringent internal accuracy requirements in the numerical integration program removed the deficiency and brought the numerical results into agreement with those of the asymptotic solution.)

The computation times for all of the solutions are significantly less than those for numerical integration and in some instances are less than the computation times of the fastest numerical approximation techniques. This computational speed makes the asymptotic solution very attractive for boundary value problems since all the numerical techniques, exact or approximate, require iterative methods to converge to a solution.

The best overall application for the asymptotic solution appears to be the midcourse application, particularly for interplanetary trajectories where μ is small. In this application the solution is convergent to second order, i. e., the second-order error is less than first order. The solution is also less subject to sensitivity problems which arise with lunar trajectories originating close to perigee or close to the moon and with interplanetary trajectories originating close to the launch planet. The lack of uniform convergence of the second order solution and the problem of sensitivity are closely associated and both have a minimum effect in the midcourse solutions.

In other applications certain boundary conditions may cause the second-order error to be larger than first order. From an examination of all the data generated (more than has been presented in Section 4) it appears that the cause of the second-order divergence, when it occurs, is not a deficiency in the second-order terms themselves, but rather the fact that the zeroth-order solution is a poor approximation to the actual trajectory. This problem is discussed several times in Section 4 and again in the next section.

The general conclusions are: (1) the second-order asymptotic solution does converge (with certain exceptions), (2) it is significantly more accurate than conic approximations, and (3) it is much faster than numerical integration.

5.2 RECOMMENDATIONS FOR FURTHER STUDY

In order to formulate a second-order asymptotic solution with more uniform accuracy, it is recommended that any further studies include the following:

    A.   A more comprehensive numerical survey which would include complete families of trajectories generated by varying each boundary

.condition through a wide range of values and, in the interplanetary cases, trajectories to several different planets. Such a survey would better define those conditions under which the different second-order solutions diverge and would indicate exactly where a better nominal or zeroth-order solution is required.

B. An analysis to determine what modifications can be made to the zeroth-order outer solution to make it a better approximation to the actual trajectory in those cases where divergence of the second-order solution does occur. This problem is discussed in some detail in Section 4, but it should be re-emphasized that (2.2-4), which is an essential condition to successful matching of the outer and inner solutions, restricts the zeroth-order solution in such a way as to have an adverse effect on the second-order accuracy. It may be possible, however, to construct a piecewise continuous zeroth-order solution from two-body arcs passing through a sequence of points obtained from the first-order solution. Only the arc closest to the target (or launch) body would have to satisfy (2.2-4) yet the total sequence, since it is obtained from the first-order solution, would be a much better approximation than the original nominal solution. Such an approach would cause some increase in computation time but should result in a uniformly valid solution for all applications, that is, a solution free of second-order divergence.

Although A and B are related, they could be carried out independently. If such is the case, then B should be given the higher priority since it would produce the more useful results.

REFERENCES

1. J. E. Lancaster. Numerical Analysis of the Asymptotic Two-Point Boundary Value Solution for Moon-to-Earth Trajectories. American Institute of Aeronautics and Astronautics Paper No. 70-1060, August 1970.

2. N. A. Carlson. An Explicit Analytic Guidance Formulation for Many-Body Space Trajectories, Massachusetts Institute of Technology PhD Dissertation, May 1969; also American Institute of Aeronautics and Astronautics Paper No. 71-117, January 1971.

3. P. R. Escobal, K. Forster, G. S. Stern, and R. J. Stern. The Hybrid Patched Conic Technique as Applied to the Lunar Trajectory Problem. Journal of the Astronautical Sciences, Vol. 16, No. 3, May—June 1969.

4. S. W. Wilson, Jr. A Pseudostate Theory for the Approximation of Three-Body Trajectories. American Institute of Aeronautics and Astronautics Paper No. 70-1061, August 1970.

5. D. V. Byrnes and H. L. Hooper. Multi-Conic: A Fast and Accurate Method of Computing Space Flight Trajectories. American Institute of Aeronautics and Astronautics Paper No. 70-1062, August 1970.

6. D. H. Novak. Virtual Mass Technique for Computing N-Body Solutions. American Institute of Aeronautics and Astronautics Paper No. 70-1057, August 1970.

7. P. E. Russell and B. Culpepper. Calculation of Trajectories Utilizing Constant and/or Slowly Varying Functions. American Institute of Aeronautics and Astronautics Paper No. 70-1076, August 1970.

8. P. E. Nacozy and T. Feagin. Chebyshev Series-Solutions of Swing-By Trajectories. American Institute of Aeronautics and Astronautics Paper No. 71-192, January 1971.

9. J. D. Cole. Perturbation Methods in Applied Mathematics. Waltham-Blaisdell Publishing Co., 1968.

10. J. E. Lancaster. Application of Matched Asymptotic Expansions to Lunar and Interplanetary Trajectories, Volume 2, Derivations of Second-Order Asymptotic Boundary Value Solutions. Final Report Contract NAS9-10526, McDonnell Douglas Astronautics Co., Feb 1972. NASA CR-2256, 1973.

11. R. H. Battin. Astronautical Guidance. McGraw Hill New York, 1964.

12. J. V. Breakwell and L. M. Perko. American Institute of Aeronautics
     and Astronautics Progress Series, Volume 17, Methods in Astro-
     dynamics and Celestial Mechanics. R. L. Duncombe and
     V. G. Szebehely, Editors, Academic Press, New York, 1966.

"The aeronautical and space activities of the United States shall be conducted so as to contribute . . . to the expansion of human knowledge of phenomena in the atmosphere and space. The Administration shall provide for the widest practicable and appropriate dissemination of information concerning its activities and the results thereof."
—NATIONAL AERONAUTICS AND SPACE ACT OF 1958

NASA SCIENTIFIC AND TECHNICAL PUBLICATIONS

TECHNICAL REPORTS: Scientific and technical information considered important, complete, and a lasting contribution to existing knowledge.

TECHNICAL NOTES: Information less broad in scope but nevertheless of importance as a contribution to existing knowledge.

TECHNICAL MEMORANDUMS: Information receiving limited distribution because of preliminary data, security classification, or other reasons. Also includes conference proceedings with either limited or unlimited distribution.

CONTRACTOR REPORTS: Scientific and technical information generated under a NASA contract or grant and considered an important contribution to existing knowledge.

TECHNICAL TRANSLATIONS: Information published in a foreign language considered to merit NASA distribution in English.

SPECIAL PUBLICATIONS: Information derived from or of value to NASA activities. Publications include final reports of major projects, monographs, data compilations, handbooks, sourcebooks, and special bibliographies.

TECHNOLOGY UTILIZATION PUBLICATIONS: Information on technology used by NASA that may be of particular interest in commercial and other non-aerospace applications. Publications include Tech Briefs, Technology Utilization Reports and Technology Surveys.

Details on the availability of these publications may be obtained from:

SCIENTIFIC AND TECHNICAL INFORMATION OFFICE

NATIONAL AERONAUTICS AND SPACE ADMINISTRATION
Washington, D.C. 20546